`UNITED STATES
NUCLEAR REGULATORY COMMISSION
WASHINGTON, D.C. 20555-0001

December 21, 2016

Mr. Edward D. Halpin
Senior Vice President and Chief
Nuclear Officer
Pacific Gas and Electric Company
P.O. Box 56
Mail Code 104/6
Avila Beach, CA 93424

SUBJECT: DIABLO CANYON POWER PLANT, UNIT NOS. 1 AND 2 - STAFF ASSESSMENT OF INFORMATION PROVIDED UNDER TITLE 10 OF THE *CODE OF FEDERAL REGULATIONS* PART 50, SECTION 50.54(f), SEISMIC HAZARD REEVALUATIONS FOR RECOMMENDATION 2.1 OF THE NEAR-TERM TASK FORCE REVIEW OF INSIGHTS FROM THE FUKUSHIMA DAI-ICHI ACCIDENT (CAC NOS. MF5275 AND MF5276)

Dear Mr. Halpin:

On March 12, 2012, the U.S. Nuclear Regulatory Commission (NRC) issued a request for information under Title 10 of the *Code of Federal Regulations*, Part 50, Section 50.54(f) (hereafter referred to as the 50.54(f) letter) (Agencywide Documents Access and Management System Accession No. ML12053A340). The request was issued as part of implementing lessons learned from the 2011 accident at the Fukushima Dai-ichi nuclear power plant. Enclosure 1 to the 50.54(f) letter requested that licensees reevaluate seismic hazards for their sites using present-day methodologies and guidance.

By letter dated March 11, 2015, Pacific Gas and Electric Company (the licensee, PG&E) responded to this request for Diablo Canyon Power Plant, Unit Nos. 1 and 2 (DCPP). The NRC staff has reviewed the information provided related to the reevaluated seismic hazard for DCPP and, as documented in the enclosed staff assessment, determined that the licensee provided sufficient information in response to Items (1) – (3), (5) – (7), and the comparison portion to Item (4) identified in Enclosure 1 of the 50.54(f) letter. Further, the NRC staff concludes that the licensee's reevaluated seismic hazard is suitable for use in the other seismic assessments associated with the 50.54(f) letter.

Contingent upon the NRC's review and acceptance of PG&E's seismic risk evaluation, including the high frequency confirmation and spent fuel pool evaluation (i.e., Items 4, 8, and 9) for DCPP, the seismic hazard reevaluation identified in Enclosure 1 of the 50.54(f) letter will be completed.

If you have any questions, please contact me at (301) 415-1617 or at Frankie.Vega@nrc.gov.

Sincerely,

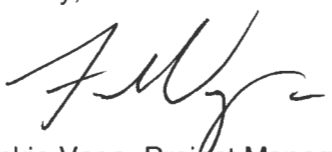

Frankie Vega, Project Manager
Hazards Management Branch
Japan Lessons-Learned Division
Office of Nuclear Reactor Regulation

Docket Nos. 50-275 and 50-323

Enclosure:
Staff Assessment of Seismic
Hazard Evaluation and Screening Report

cc w/encl: Distribution via Listserv

STAFF ASSESSMENT BY THE OFFICE OF NUCLEAR REACTOR REGULATION

RELATED TO SEISMIC HAZARD AND SCREENING REPORT

DIABLO CANYON POWER PLANT UNIT NOS. 1 AND 2

DOCKET NOS. 50-275 AND 50-323

1.0 INTRODUCTION

By letter dated March 12, 2012 (NRC, 2012a), the U.S. Nuclear Regulatory Commission (NRC or Commission) issued a request for information to all power reactor licensees and holders of construction permits in active or deferred status, pursuant to Title 10 of the *Code of Federal Regulations* (10 CFR), Section 50.54(f), "Conditions of Licenses" (hereafter referred to as the "50.54(f) letter"). The request was issued in connection with implementing lessons-learned from the 2011 accident at the Fukushima Dai-ichi nuclear power plant, as documented in the NRC's Near-Term Task Force (NTTF) report (NRC, 2011a). Recommendation 2.1 in that document recommended that the NRC staff issue orders to all licensees to reevaluate seismic and flooding hazards for their sites against current NRC requirements and guidance. Subsequent staff requirements memoranda associated with SECY-11-0124 (NRC, 2011c) and SECY-11-0137 (NRC, 2011d) directed the NRC staff to issue requests for information to licensees pursuant to 10 CFR 50.54(f) to address this recommendation.

Enclosure 1 to the 50.54(f) letter requests that addressees perform a reevaluation of the seismic hazards at their sites using present-day NRC requirements and guidance to develop a ground motion response spectrum (GMRS).

The required response section of Enclosure 1 requests that each addressee provide the following information:

(1) Site-specific hazard curves (common fractiles and mean) over a range of spectral frequencies and annual exceedance frequencies;

(2) Site-specific, performance-based GMRS developed from the new site-specific seismic hazard curves at the control point elevation;

(3) Safe shutdown earthquake (SSE) ground motion values, including specification of the control point elevation;

(4) Comparison of the GMRS and SSE. A high-frequency evaluation (if necessary);

(5) Additional information, such as insights from NTTF Recommendation 2.3 walkdown and estimates of plant seismic capacity developed from previous risk assessments, to inform NRC screening and prioritization;

(6) Interim evaluation and actions taken or planned to address the higher seismic hazard relative to the design basis, as appropriate, prior to completion of the risk evaluation (if necessary);

(7) Selected risk evaluation approach (if necessary);

(8) Seismic risk evaluation (if necessary); and

(9) Spent fuel pool (SFP) evaluation (if necessary).

Present-day NRC requirements and guidance for characterizing seismic hazards use a probabilistic approach in order to develop a risk-informed, performance-based GMRS for the site. Regulatory Guide (RG) 1.208, "A Performance-based Approach to Define the Site-Specific Earthquake Ground Motion" (NRC, 2007), describes an acceptable approach. As described in the 50.54(f) letter, if the reevaluated seismic hazard, as characterized by the GMRS, is not bounded by the current plant design-basis SSE, further seismic risk evaluation of the plant is merited.

By letter dated November 27, 2012 (Keithline, 2012), the Nuclear Energy Institute (NEI) submitted Electric Power Research Institute (EPRI) report "Seismic Evaluation Guidance: Screening, Prioritization, and Implementation Details (SPID) for the Resolution of Fukushima Near-Term Task Force Recommendation 2.1 Seismic" (EPRI, 2012), hereafter called the SPID. The SPID provides guidance to support licensees when responding to the 50.54(f) letter in a manner that will address the Requested Information Items in Enclosure 1 of the 50.54(f) letter. By letter dated February 15, 2013 (NRC, 2013a), the NRC staff endorsed the SPID.

The required response section of Enclosure 1 to the 50.54(f) letter specifies that Western U.S. (WUS) licensees will provide their Seismic Hazard and Screening Report (SHSR) within 3 years after issuance of the 50.54(f) letter. The WUS licensees were granted an additional year to submit the SHSRs because their sites could not use the updated EPRI seismic ground motion models and seismic source characterization (SSC) models for the Central and Eastern U.S. (CEUS) (NRC, 2012b; EPRI, 2012). As specified in Enclosure 1 to the 50.54 (f) letter, the WUS licensees used the Senior Seismic Hazards Advisory Committee (SSHAC) Level 3 process to develop the ground motion characterization (GMC) and SSC models necessary for the more complex geology at WUS sites.

Industry also proposed that licensees perform an expedited assessment, referred to as the Augmented Approach, for addressing the requested interim evaluation (Item 6 above), which would use a simplified assessment to demonstrate that certain key pieces of plant equipment for core cooling and containment functions, given a loss of alternating current (ac) power, would be able to withstand a seismic hazard up to two times the design basis. By letter dated April 9, 2013 (Pietrangelo, 2013), the Nuclear Energy Institute (NEI) provided a revision to the 50.54(f) letter schedule for plants needing to perform: (1) the Augmented Approach by implementing the Expedited Seismic Evaluation Process, and (2) a seismic risk evaluation. By letter dated May 7, 2013 (NRC, 2013b), the NRC determined that the modified schedule was acceptable.

2.0 REGULATORY BACKGROUND

The structures, systems, and components important to safety in operating nuclear power plants are designed either in accordance with, or meet the intent of Appendix A to 10 CFR Part 50, General Design Criteria (GDC) 2; "Design Bases for Protection Against Natural Phenomena" and Appendix A to 10 CFR Part 100, "Reactor Site Criteria." GDC 2 states that structures, systems, and components important to safety at nuclear power plants shall be designed to withstand the effects of natural phenomena such as earthquakes, tornadoes, hurricanes, floods, tsunami, and seiches without loss of capability to perform their safety functions.

For initial licensing, each licensee was required to develop and maintain design bases that, as defined by 10 CFR 50.2, identify the specific functions that structures, systems, or components of a facility must perform, and the specific values or ranges of values chosen for controlling parameters as reference bounds for the design. The design bases for the structures, systems, and components reflect appropriate consideration of the most severe natural phenomena that had been historically reported for the site and surrounding area. The design bases are also to reflect sufficient margin to account for the limited accuracy, quantity, and period of time in which the historical data have been accumulated.

The seismic design bases for currently operating nuclear power plants were either developed in accordance with, or meet the intent of, GDC 2 and 10 CFR Part 100, Appendix A. Although the regulatory requirements in Appendix A to 10 CFR Part 100 are fundamentally deterministic, the NRC regulations in 10 CFR Part 52 for determining the seismic design-basis ground motions for new reactor applications after January 10, 1997, requires that uncertainties be addressed through an appropriate analysis, such as a probabilistic seismic hazard analysis (PSHA), as described in 10 CFR 100.23.

Section 50.54(f) of 10 CFR states that a licensee shall at any time before expiration of its license, upon request of the Commission, submit written statements, signed under oath or affirmation, to enable the Commission to determine whether or not the license should be modified, suspended, or revoked. On March 12, 2012, the NRC staff issued requests for licensees to reevaluate the seismic hazards at their sites using present-day NRC requirements and guidance, and identify actions planned to address plant-specific vulnerabilities associated with the updated seismic hazards.

2.1 Screening Evaluation Results

The Diablo Canyon Power Plant, Unit Nos. 1 and 2 (DCPP) has several different response spectra that were used in the seismic design of Units 1 and 2. By letter dated April 29, 2013 (PG&E, 2013a), Pacific Gas and Electric Company (PG&E, the licensee) clarified that the double design earthquake (DDE) corresponds to the SSE for DCPP. By letter dated March 11, 2015 (PG&E, 2015a), the licensee provided its SHSR for the DCPP site. The licensee's SHSR concluded that the site GMRS exceeds the DDE (i.e., the SSE) for the DCPP site within the frequency range of 1 Hertz (Hz) to 10 Hz. Therefore, the licensee will perform a risk evaluation. Because the GMRS exceeds the SSE above 10 Hz the risk evaluation will include a high frequency confirmation. Further, the licensee indicated that it will perform a SFP evaluation.

On May 13, 2015 (NRC, 2015a), and October 27, 2015 (NRC, 2015b), the NRC staff issued letters providing the outcome of its screening and prioritization evaluation for WUS plants. As indicated in the letters, the NRC staff confirmed the licensee's screening results and examined key parameters to prioritize plants for completing seismic risk evaluations. These prioritization parameters included: (1) the maximum ratio of the reevaluated hazard (i.e., GMRS) to the SSE in the 1–10 Hz range; (2) the maximum ground motion in the 1–10 Hz range; and (3) insights from previous seismic risk evaluations. As such, Group 1 plants are generally those that have the highest reevaluated hazard relative to the original plant seismic design-basis (i.e., GMRS to SSE), as well as ground motions in the 1–10 Hz range that are generally higher in amplitude. Based on these criteria, the DCPP is prioritized as a Group 1 plant and is expected to conduct a seismic risk evaluation that will be submitted to NRC by September 30, 2017.

The NRC staff issued requests for additional information (RAIs) on June 29, 2015 (NRC, 2015c), August 27, 2015 (NRC, 2015d), October 1, 2015 (NRC, 2015e), and November 13, 2015 (NRC, 2015f). The licensee provided its responses to these RAIs on August 12, 2015 (PG&E, 2015b), September 16, 2015 (PG&E, 2015c), and December 21, 2015 (PG&E, 2015d). This additional information is also included in the NRC staff's review of the licensee's SHSR submittal.

3.0 TECHNICAL EVALUATION

The NRC staff evaluated the licensee's submittal to determine if the provided information responded appropriately to Enclosure 1 of the 50.54(f) letter with respect to characterizing the reevaluated seismic hazard. In addition to an evaluation of the technical information, the NRC staff also determined if the process used to develop the reevaluated seismic hazard was acceptable and consistent with applicable guidance.

3.0.1 Summary of Regional Seismotectonic Setting

The DCPP is located in the Irish Hills along the central California coast in the coastal flank of the San Luis Range. The San Luis Range is one of several ranges in central California that compose the California Coastal Ranges. These ranges are fault-bounded bedrock blocks that are being slowly uplifted in response to transpressional stresses generated by the differential tectonic motions of the North American and Pacific plates (Lettis and Hanson, 1991; Lettis and Hall, 1994; McLaren and Savage, 2001). The transpressional stress comprises simultaneous NNW-SSE right-lateral (clockwise) horizontal shear and north east-south west (NE-SW) compression oriented at roughly ninety degrees to the North American-Pacific plate boundary. Most of the resulting tectonic deformation is manifested as right-lateral strike-slip motion between the North American and Pacific plates, primarily along the San Andreas Fault. The San Andreas fault runs subparallel to the California coastline, but is located approximately 80 kilometer (km) inland from the DCPP (see Figure 3.0-1 of this staff assessment). The remaining component of horizontal motion occurs as right-lateral slip on a series of coast-parallel strike-slip faults nearer to the DCPP, including the Hosgri and Shoreline faults (Atwater, 1989; Argus and Gordon, 2001; Lettis et al., 2004). Within the regional tectonic setting, the Hosgri fault forms the southernmost segment of the 410 km-long San Gregorio-San Simeon-Hosgri fault system. The compressional component of transpressional stress is accommodated by oblique-

slip and reverse-slip faulting on block-bounding NW-SE trending faults that uplifted crustal blocks of the Coast Ranges, including the San Luis Range. Within this tectonic setting, the Southwest Boundary fault zone and Los Osos faults accommodate this uplift.

Earthquake focal mechanisms in south central California (see Figure 3.0-1 of this staff assessment) are mainly reverse and strike-slip, consistent with right-lateral transpression (e.g., McLaren and Savage, 2001; Hardebeck, 2010). In particular, focal mechanisms and the spatial distribution of seismic events along the Hosgri fault in the subsurface are predominantly right-lateral strike-slip on a nearly vertical to steeply east-dipping fault zone, with active seismicity to a depth of about 12 km (McLaren and Savage, 2001; Hardebeck, 2010; McLaren et al., 2008). A similar distribution of hypocenters illuminates the Shoreline fault. There is also relatively abundant seismicity recorded beneath the DCPP and to the east of the Hosgri fault with both reverse and strike-slip focal mechanisms. However, the rates of seismicity diminish considerably west of the Hosgri fault within the Santa Maria Basin. The 2003 **M**6.5 San Simeon earthquake, which was one of the largest recorded earthquakes in the central California Coastal Ranges (see Figure 3.0-1 of this staff assessment), was primarily a reverse-faulting event that resulted from right-lateral transpression. McLaren et al. (2008) concluded that the fault patterns illuminated by the main shock, which was located approximately 40 km NNW from the DCPP, and aftershocks showed well-defined reverse slip on the Oceanic fault with antithetic back-thrusting, resulting in uplift of the Santa Lucia Range as a popup block.

Global Positioning System (GPS) data also show right-lateral shear and plate-normal convergence (DeMets, 2012; DeMets et al., 2014; Murray, 2012; Bird, 2012). Based on the GPS data, the total horizontal slip budget available for faults west of the Oceanic fault is 1–3 mm/yr. Plate-normal rates are significantly lower, on the order of 0.2–0.5 mm/yr. For comparison, horizontal slip of the San Andreas Fault in central California is estimated to be 25–36 mm/yr (e.g., Sieh and Jans, 1984; Titus et al., 2005; Toké et al., 2011; Titus et al., 2011).

3.0.2 Summary of Local Geology and Site Area Faults

The DCPP is located on a relatively broad Quaternary terrace surface near the mouth of Diablo Canyon Creek. Bedrock geology of the site consists of the Miocene (5–23 million years ago) Obispo Formation, which is a 400 m thick sequence of thin to thickly-bedded marine volcanic and volcaniclastic deposits. Beneath the DCPP site, the Obispo Formation has been both faulted and folded and typically dips 35° to 75° to the north (Hall, 1973). A thin veneer of marine sands and gravels (typically 1- to 2-meters thick) underlain by a relatively thick sequence of nonmarine fluvial sands and gravels and colluvium (1 meter thick to several tens of meters thick) overlies the Obispo Formation. The basal contact between the overlying marine sands and gravels and the underlying Obispo Formation is a gently southwest-sloping eroded marine terrace platform. This eroded platform can be very sharp and planar or have considerable relief, depending on the resistance of the beds within the Obispo Formation.

Based on surface geologic mapping, the structure of the Irish Hills is a syncline cored by Tertiary age (2.6–65 million years ago) rocks of the Obispo, Monterey, and Pismo Formations. The Obispo Formation rests unconformably above highly deformed bedrock, including the Jurassic (144–200 million years ago) Franciscan Formation. The Franciscan Formation is a chaotic mélange of basaltic volcanic rocks (many of which have been altered to greenstone),

radiolarian chert, sandstone, limestone, serpentinite, shale, and high-pressure metamorphic rocks. This diverse mix of rock types makes it difficult to accurately decipher geologic features in the subsurface, especially folds and faults.

An important geological dataset used to interpret the recent tectonic and seismic history of the DCPP site is the marine terraces and their associated wave-cut platforms and paleoshorelines. These marine terraces develop at the shoreline impact zone, as waves cut into and erode rocks along the beach line. The identification and dating of these marine terraces in the DCPP region, coupled with the known chronology of sea-level elevations during different sea-level "stands" (i.e., periods of time when the sea level was stable long enough for a platform to be developed), allow geologists to estimate the uplift rates of the fault-bounded blocks of the California Coastal Ranges, including the San Luis Range and the Irish Hills. The location, elevation, geomorphic characteristics, and ages of these features were mapped in detail by Hanson et al. (1994) and by PG&E as part of the Long-Term Seismic Program (PG&E, 1988, 1991a). These studies showed that the uplift rate for the Irish Hills is approximately 0.2 mm/yr, compared to a lower uplift rate of less than 0.1 mm/yr for areas south of the DCPP, including San Luis Bay.

As further addressed in Section 3.3 of this staff assessment, the faults that are most significant to the seismic hazard at the DCPP are the Hosgri, Los Osos, San Luis Bay (within the Southwestern Boundary fault zone), and Shoreline faults. Other named faults that were included in the SSC evaluation are the Wilmar Avenue, Oceano, Casmalia, San Miguelito, Edna, West Huasna, and Rinconada faults. The surface traces of these faults are shown in Figure 3.0-2 of this staff assessment.

The Hosgri fault is located just a few kilometers offshore of south-central California and forms the eastern boundary of the offshore Santa Maria Basin (PG&E, 1988; Clark et al., 1991; Steritz and Luyendyk, 1994). Characterization of the fault is primarily derived from traditional marine seismic reflection data and single-channel, high-resolution sparker data. The Hosgri fault has been mapped along its entire length using petroleum industry multichannel seismic-reflection data that images the traces of the fault to 3 km depth beneath the seafloor (PG&E, 1988, 1991a; Willingham et al., 2013). Significant sections of the Hosgri fault also were remapped using single-channel, high-resolution U.S. Geological Survey (USGS) sparker data (Johnson and Watt, 2012; PG&E, 2014). In the immediate vicinity of the DCPP, the Hosgri fault trends N 25° to N 30° W and comprises multiple fault traces, with individual segment lengths up to 18 km long that overlap *en-echelon*, forming a fault zone up to 2.5 km wide. In the seismic reflection profiles, fault traces appear to be vertical to steeply dipping in the uppermost sedimentary section, but some of the fault traces below about 1 km depth appear to be subvertical or dipping steeply to the east.

The Shoreline fault is a 16–23 km-long fault that bounds most of the western margin of the Irish Hills. At its closest approach, the fault is located approximately 600 m from the DCPP. The fault was identified from a number of geological and geophysical observations, including the nearly vertical alignment of earthquake hypocenters (Hardebeck, 2013) that coincides with linear magnetic anomalies revealed as part of the high-resolution aeromagnetic data (e.g., Langenheim et al., 2009). High-resolution two-dimensional and three-dimensional seismic imaging data within the San Luis Bay further supports the location and lateral extent of the Shoreline fault (PG&E, 2011; 2014). The NRC staff previously reviewed much of the geological

and geophysical information characterizing the Shoreline fault as part of a deterministic seismic hazard evaluation (NRC, 2012c).

The Los Osos fault, located about 10 km north-northeast (NNE) of the DCPP, is mapped as a southwest dipping, reverse or right-oblique fault that separates the uplifted San Luis-Pismo block to the southwest from the lower terrane of the Cambria block to the northeast. Its surface trace is a series of discontinuous subparallel fault strands that extend from an intersection with the Hosgri fault in Estero Bay in the north to an intersection with the West Huasna fault southeast of the city of San Luis Obispo.

The Southwestern Boundary zone is a collection of reverse and oblique reverse-strike-slip faults that collectively uplift the San Luis-Pismo block from the subsiding Santa Maria Valley. This zone of faults, which includes the San Luis Bay fault, is 4–10 km wide and extends from the northwest at the intersection of the San Luis Bay fault with the Shoreline or Hosgri faults to the southeast, where this zone of faults is inferred to merge with the Oceanic-West Huasna fault zone along the western base of the San Rafael Range.

3.0.3 Senior Seismic Hazards Analysis Committee Approach

Consistent with current NRC guidance, the licensee used SSHAC Level 3 studies to develop both the SSC and GMC models for the DCPP site (PG&E, 2015e; GeoPentech, 2015). Similar to the SSHAC Level 3 studies developed for the Palo Verde Nuclear Generating Station; the SSHAC Level 3 studies for the DCPP include a site-specific SSC model, but rely on a GMC model that was developed within the Southwestern United States (SWUS) Ground Motion Characterization Project. The SWUS project was sponsored by both PG&E and Arizona Public Service.

The SSHAC process was developed as a formal approach that incorporates expert judgment to evaluate uncertainties in a PSHA for nuclear power plants (Budnitz et al., 1997). The process allows for the consideration of the complete set of seismological, geological, and geophysical data, models, and methods that exists within the larger technical community, which are relevant to the seismic hazard analysis. In the SSHAC process, technical experts evaluate and integrate available data, models, and methods into the PSHA to ensure that the hazard results capture the center, body, and range of technically-defensible interpretations (i.e., consider the range of diverse technical interpretations from the larger technical community) (NRC, 2012c).

Site-specific hazard curves and associated seismic engineering inputs (e.g., GMRS or design spectra) are derived from three component studies: SSC, GMC, and site response. The SSC and GMC models, developed through the SSHAC studies, provide the inputs to the PSHA. The models are represented by logic trees, with weighted branches that account for epistemic uncertainty (i.e., uncertainty attributable to incomplete knowledge about a phenomenon). A fundamental aspect of the SSHAC methodology is the distinct and separate treatment of epistemic and aleatory uncertainty (i.e., uncertainty inherent in a random phenomenon). The outputs from the PSHA are a suite of probabilistic hazard curves (i.e., peak ground acceleration and spectral ground accelerations) for either a reference rock or soil condition. Section 3.1 of this staff assessment evaluates the SSC, and the GMC is evaluated in Section 3.2. The PSHA

is reviewed in Section 3.3. Site response for the DCPP, which was not developed using a SSHAC process, is evaluated in Section 3.4 of this staff assessment.

As requested in the 50.54(f) letter (NRC, 2012a), the licensee conducted SSHAC Level 3 studies for both the SSC and GMC using the guidance in NUREG/CR-6372 (Budnitz et al., 1997) and NUREG-2117 (NRC, 2012c). The licensee served as project sponsors for the SSC component of the SSHAC, while both PG&E and Arizona Public Service co-sponsored the GMC. These respective licensees identified the Project Technical Integrators (PTIs), who were the technical leads for the SSC and GMC. Technical Integration Teams (TI Teams) developed and documented the SSC and GMC models. In addition, the TI Team members served as both evaluator and integrator experts during the SSHAC process.

The SSHAC studies for both the SSC and GMC followed the same fundamental process. The TI Team developed a project plan and began compiling a project database. The TI Team then organized a series of workshops to discuss applicable data and models. Initial workshop(s) focused on the compilation and development of data needed to support the models, which were identified by resource experts. Subsequent workshop(s) focused on development of models and consideration of alternative models, which were supported by proponent experts. Observers, including NRC staff, also attended the workshops along with Participatory Peer Review Panel (PPRP) members. The TI Team then developed preliminary models, and performed initial hazard calculations and sensitivity analyses. These preliminary insights were discussed at an additional workshop, and the TI Team adjusted the models based on feedback from this workshop and additional discussions with the PPRP. The TI Team conducted the final hazard calculations and sensitivity analyses, and documented the results of the SSHAC in a final project report (PG&E, 2015e).

An important part of a SSHAC Level 3 process is a PPRP, which provides peer review and feedback to the TI Teams throughout the evaluation. The PPRP attended workshops and working meetings, reviewed work products, and provided input to the TI Teams throughout SSC and GMC development. The PPRP also provided a formal review of the resulting hazard study (Appendix B, PG&E, 2015e). In addition, the project management teams at the DCPP and within the SWUS project developed an electronic library of workshop materials for the SSHAC participants, which included workshop summaries, presentations, references, and data.

Additional details about the SSHAC process are discussed and evaluated in the following sections of this staff assessment, in the context of technical topics for the SSC and GMC development. In each subject area, the reviews identify the most significant technical issues for the PSHA, and discuss how the NRC staff evaluated these issues.

3.1 Seismic Source Characterization

The SSC for the DCPP (PG&E, 2015e) site represents the first stage of a PSHA. The TI Team's goal was to develop an SSC model for the PSHA based on evaluation of available geological, geophysical, and seismological information. For the SSC, the TI Team considered two types of seismic sources: faults and areal source zones. The SSC TI Team developed input parameters for these seismic sources from: (1) earthquake records, based on the instrumented and historical seismicity catalogued for the region; (2) geologic evidence of the

magnitude, age, and frequency of past seismic events; (3) geological and geophysical evidence for the location and geometry of faults; (4) geological and geophysical evidence to constrain the amount and timing of fault slip; and (5) geophysical evidence to determine the nature of tectonic stresses and to quantify the resulting crustal strain, largely based on GPS measurements.

3.1.1 Assessments of the SSHAC Process for SSC

To develop the SSC for the DCPP site, the TI Team first compiled existing information from plant licensing documents, the extensive record of information acquired as part of the on-going Long-Term Seismic Program, information acquired through cooperative activities with other governmental agencies such as the California Coastal Commission, academic institutions, the USGS, and published technical information. This compilation helped focus the first SSHAC workshop (held November 29–December 1, 2011) on identifying data needs, which considered a range of presentations from resource experts. The resource experts provided summaries of available data sets to assist in addressing significant issues, including legacy data from the prior Long-Term Seismic Program studies (PG&E, 1988). Hazard results from prior PSHA studies, especially the PSHA developed by PG&E for the Shoreline fault zone study (PG&E, 2011), provided the basis to inform and focus the discussions of data needs on the most hazard significant issues. Based on the discussions during the first workshop, the TI Team recognized the need to conduct additional studies to improve the characterization of fault geometries in the subsurface and to develop information on Quaternary (i.e., less than 2.6 million years ago) deformation and slip rates on the fault sources. Following the first workshop, significant new information was provided to the TI Team, especially because of the significant new seismic imaging program that was being conducted for the California Coastal Commission Seismic Imaging Project (CCCSIP) (PG&E, 2014).

The second SSHAC workshop (held November 6–8, 2012) focused on developing models and associated data that were most significant to seismic hazards at the DCPP site. For the second SSHAC workshop, multiple experts were queried for data and model information, including information about data gaps and alternative interpretations of the available information, from which several technical challenges emerged regarding development of SSC models for the PSHA. These key technical challenges included: (1) how to treat multi-fault ruptures that could lead to very large earthquake magnitudes, especially as envisioned in the State of California's Uniform California Earthquake Rupture Forecast v.2 (UCERF2) model (Field et al., 2009); (2) the tectonic forces driving the uplift of the Irish Hills, and whether or not to project a blind thrust fault beneath the Irish Hills; (3) the use of relocated hypocenters in distinguishing fault sources or areal source zones; (4) sensitivity of the PSHA results to the choice of a magnitude scaling relationship; and (5) whether or not to include the potential for non-Poissonian (i.e., time-dependent) earthquake recurrence.

At the third SSHAC workshop (held March 25–27, 2014), the TI Team presented the preliminary SSC model with an emphasis on obtaining feedback from the PPRP. The TI Team described the technical bases for the models to allow for a reasoned discussion of the constraints interpreted from the available data. The main topics of discussion for the SSC model focused on the potential for non-Poissonian earthquake recurrence, conceptual development of linked fault ruptures, slip rate allocation models, and magnitude-distribution models. In addition, resource experts provided updates to the CCCSIP onshore and offshore investigations. Much

of the interaction between the PPRP and TI Team centered on the basis for developing SSC logic trees and associated weighting schemes, including consideration of alternative models and data uncertainties. The PPRP also used the hazard sensitivity analyses to focus the TI Team's attention on further refining data and models that had the greatest potential contribution to the resulting PSHA at the DCPP site.

Several analyses on specific elements of the SSC model were incomplete at the third workshop, including implementation of alternative magnitude-frequency distributions and the time-dependence uncertainty model for fault sources. These incomplete analyses in the SSC model were identified to the PPRP during the workshop, and required subsequent presentations to the PPRP after the conclusion of the third workshop. These working meetings were held in July and October of 2014.

After reviewing the preliminary SSHAC report, the PPRP provided extensive comments to the TI Team and then reviewed the TI Team's responses. In summary, the PPRP concluded in its endorsement letter (PG&E, 2015e, Appendix B):

> Based on our observation of the completeness and professional standard by which the evaluation and integration activities were conducted, the Panel concludes that the data, models, and methods within the larger technical community have been properly evaluated, and that the center, body, and range of technically defensible interpretations have been appropriately represented in the SSC model. Accordingly, the Panel concludes that both the process and technical aspects of the DCPP SSC assessment fully meet accepted guidance and current expectations for a SSHAC Level 3 study.

STAFF EVALUATION

Based on observations made during the SSHAC workshops and review of the SSHAC documentation, the NRC staff concludes that the licensee conducted the SSHAC workshops in a manner that is consistent with applicable NRC guidance. In addition, the NRC staff does not find significant departures from the guidance in the approach used by the TI Team to develop the SSC model. Due to the potential for anchoring to previous models, the TI Team addressed the potential for cognitive bias during each workshop. The PPRP also discussed sensitivity to cognitive bias as part of the SSHAC process and addressed this in their review. An important component of the SSHAC process is complete documentation. Based on its review, the NRC staff concludes that the SSHAC documentation (PG&E, 2015e) provides an acceptably complete record of the approach used to develop the SSC model. Based on observations made during the SSHAC workshops and review of the SSHAC documentation, the NRC staff also concludes that a reasonable range of resource and proponent experts were engaged in the SSHAC workshops; and that a broad range of alternative data and models were considered. The NRC staff used these observations, and their knowledge of the geology and seismology of the DCPP site region, to conclude that the TI Team took appropriate steps to ensure that the resulting SSC model captures the center, body, and range of the technically-defensible interpretations.

The success of a SSHAC Level 3 depends strongly on the effective review and engagement of the PPRP with the TI Team. To evaluate the effectiveness of the PPRP for the SSC model development, the NRC staff reviewed the PPRP and TI Team correspondence, including comment and response logs, and observed workshop interactions. The NRC staff observed open dialog between the TI Team and the PPRP at workshop meetings, which included several significant comments or suggestions from the PPRP that required appreciable effort by the TI Team to resolve. The NRC staff also observed that the PPRP members were well engaged after the third workshop to ensure that the technical aspects of the final SSC model that were not included in the workshop discussions were sufficiently justified and fully documented. Moreover, during the duration of the project, one or more members of the PPRP attended many of the 36 working meetings as observers. The NRC staff concludes that the PPRP was effective and engaged throughout the SSC SSHAC study and that there were no unresolved PPRP issues at the end of the project, as fully described in the PPRP closure letter (PG&E, 2015e).

In summary, based on the NRC staff's review of the SSHAC documentation, observations made at SSHAC workshops, and knowledge of the geological and seismological characteristics of the DCPP region, the NRC staff concludes that the licensee acceptably implemented a SSHAC Level 3 process to develop the SSC model.

3.1.2 Summary of SSC Database

As described in Chapter 4 of the SSC SSHAC report (PG&E, 2015e), the SSC SSHAC study relied on a database that consisted of several generations of data and related technical information. In response to License Condition 2.C.(7), which was imposed on PG&E by the NRC when the operating license for Unit 1 was issued in 1984, PG&E reevaluated the seismic design bases of the DCPP. As part of the ensuing Long-Term Seismic Program, PG&E committed to an ongoing effort to study seismic issues and to perform periodic seismic reviews of the DCPP (PG&E, 1991b and 1991c). To date, data acquisition for the Long-Term Seismic Program has included: (1) earthquake records from seismic monitoring, including the PG&E Central Coast Seismic Network; (2) high-resolution potential field data (magnetics and gravity); (3) seismic reflection data; (4) bathymetric measurements; and (5) topographic data.

This commitment to ongoing research and review included the CCCSIP offshore and onshore studies, independent research by USGS investigators under the PG&E–USGS Cooperative Research and Development Agreement (CRADA) program, studies funded by PG&E to university researchers and consultants, and independent research by university researchers and the California Geological Survey (CGS). Through the CRADA program, important geological, geophysical, and seismological data were acquired from 2008 through 2011, with an emphasis on characterizing the Shoreline fault (PG&E, 2011). In addition to recompiled and new onshore and offshore gravity and magnetic surveys, this data set included updates to the geological maps of the DCPP site, new high-resolution single-channel reflection profiles (Sliter et al., 2010), and multi-beam echo-sounder (MBES) surveys of the seafloor bathymetry in the nearshore regions from Estero Bay to San Luis Obispo Bay. The MBES data were acquired by the Seafloor Mapping Lab at the California State University Monterey Bay (CSUMB, 2012).

In 2006, California Assembly Bill 1632 directed the California Energy Commission to assess, among other things, the potential vulnerability of the DCPP to a major disruption due to a seismic event. To support this assessment, PG&E collected additional onshore and offshore geophysical data to reduce uncertainties in the characterization of seismic sources, using current state-of-the-practice methods and approaches. This geophysical program began in 2011 and ended in 2014, and included both two-dimensional (2D) and three-dimensional (3D) seismic reflection data in the offshore and onshore regions near the DCPP (PG&E, 2014). Within this phase of data collection, PG&E collected a significant amount of new onshore and off-shore seismic images from 2D- and 3D-low energy seismic signals (LESS) (PG&E, 2014). Specifically, the LESS surveys were designed to image near-surface features of the Hosgri fault north of Point Buchon, and the Shoreline fault in San Luis Bay. In addition, PG&E acquired high-resolution tomographic data within a 1 km^3 volume directly beneath the DCPP site. This high-resolution seismic tomographic data provides a detailed characterization of compressional-wave and shear-wave velocity structure beneath the DCPP, which was used in the site response analysis (Section 3.4 of this staff assessment).

In 2012, the USGS acquired additional high-resolution multibeam images of the Hosgri fault in Estero Bay (Hartwell et al., 2013). As part of this survey, the USGS remapped a linear southwest-facing bathymetric slope, which is referred to as the cross-Hosgri-slope. This feature is important because it provides one of the constraints on the slip rate of the Hosgri fault. Johnson et al. (2014) interprets this feature as the shoreface of a Pleistocene (i.e., the period between 11,500 years ago and 2.5 million years ago) sand spit that has been offset by strike-slip motion on the Hosgri fault.

Through the CRADA program, the USGS also compiled a database of earthquake hypocenter and focal mechanism data that were used to support fault characterizations (Hardebeck, 2010, 2013). Within this set of studies, refinements were made to the locations of the earthquake hypocenters based on an advanced technique called double-difference tomography to develop a 3D crustal velocity model (Zhang and Thurber, 2003).

In addition to the aforementioned datasets, the database developed for the SSC SSHAC study by PG&E included new geologic mapping and geomorphic analysis to support the TI Team's characterization of the Los Osos, Cambria, and San Luis Bay faults, including constraints on fault slip rates. These data included updates to fluvial and marine terrace characterizations, revised geologic maps, and subsurface data compiled from oil and gas wells, CalTrans wells, and existing geotechnical studies. This information is detailed in the CCCSIP Report (PG&E, 2014).

STAFF EVALUATION

The success of the SSHAC process in developing the center, body, and range of technically defensible interpretations begins by providing the TI Team with a broad range of geological, geophysical, and seismological information. The project database includes the extensive geological, geophysical, and seismological information that has been collected since the initiation of the Long-Term Seismic Program in 1984, in addition to new data that were collected as part of the SSHAC study and in response to the data issues identified at the first Workshop. The NRC staff previously reviewed much of these data during extensive technical interactions

with the licensee. This includes the staff's review of the Long-Term Seismic Program that is documented in NUREG-0675, Supplement No. 34 (NRC, 1991), which concluded that PG&E met the requirements of License Condition 2.C(7). In addition, the staff reviewed the PG&E Shoreline Report (PG&E, 2011), which is documented in Research Information Letter 12-01 (NRC, 2012c). Moreover, the NRC staff observed that many of the proponent models that were provided at the second workshop relied extensively on the same data. Based on the NRC staff's observations at the SSHAC workshop, prior NRC technical evaluation of much of this data, and careful review of the summary of data provided in Chapter 4 of the SSC SSHAC report (PG&E, 2015e); the NRC staff concludes that the licensee assembled an adequate database necessary for a SSHAC SSC study, which is up-to-date and includes an appropriate range of geological, geophysical, and seismological information.

Moreover, in conducting the technical review for this staff assessment, the NRC staff relied on a subset of the seismic imaging data to independently evaluate the slip rate of the Hosgri fault. The details of this portion of the staff's review are described in Section 3.1.4.2 of this staff assessment. For this independent evaluation of the Hosgri fault, the staff used an aggregation of offshore seismic data from Southern Estero Bay that included the USGS 2008–2009 high-resolution sparker tracklines and the 1986 joint PG&E and Alaska COMAP lines.

3.1.3 SSC Modeling Approach for Seismic Sources

As described in Chapter 6 of the SSC SSHAC report (PG&E. 2015e), the TI Team developed an overall logical framework to evaluate active faults and associated faulting characteristics, including fault slip, fault rupture, and faulting recurrence. In this overall framework, the TI Team developed both fault and areal sources. The TI Team defines fault sources as representations of well-defined and geologically mapped seismogenic fault zones. Fault sources are characterized by the TI Team based on their location, geometry, depth extent, slip sense, slip rate, magnitude-frequency distribution, and probability of occurrence of an earthquake in a given time period. The TI Team categorized the fault sources as primary faults (Hosgri, Shoreline, Los Osos, and San Luis Bay faults), connected faults (local and regional faults that directly connect to the primary faults as part of a potentially complex fault rupture), the San Andreas fault, and other regional faults, including those derived from the UCERF3 model (Field et al., 2013).

Areal sources are defined by an areal source boundary, maximum magnitude earthquakes (M_{max}), and magnitude-frequency distributions. Within the areal source that encompasses the DCPP, the TI Team used a series of virtual faults to model the source zone seismicity. For the other areal source zones, the TI Team modeled the occurrence of earthquakes as point sources. The details of the areal source zone characterization and staff's review of the areal sources is provided in Section 3.1.5 of this staff assessment.

The essential logical element of the TI Team's approach to developing SSC models is that earthquakes in transpressive tectonic environments (such as the DCPP site) often involve complex ruptures on several connected faults. This assessment was derived by the TI Team from an evaluation of the fault rupture patterns on nine historical earthquakes in regions with transpressive tectonic settings that are similar to the tectonic setting at the DCPP site. Based on these analogs, the TI Team eschewed traditional PSHA fault-source characterization of

individual faults in favor of multi-fault models that they considered to explicitly account for the inherent complexities and constraints of connected fault ruptures.

First, the TI Team developed fault geometry models to capture the range in each of the primary fault's geometric characteristics (e.g., length, dip, down-dip width). For example, the TI Team developed three alternative fault geometry models for the Hosgri fault to account for uncertainty in fault dip, which ranged between 75 and 90 degrees. The TI Team lumped the three remaining primary faults (Los Osos, San Luis Bay, and Shoreline) into a single group of faults that were referred to as the San Luis Pismo Block (SLPB). For the SLPB, the TI Team then developed three alternative fault-geometry models (i.e., Outward Vergent, Southwest Vergent, and Northeast Vergent) to account for the alternative interpretations in how uplift of the San Luis Range occurs geologically through different combinations of thrust, reverse, and oblique strike-slip faulting on these three SLPB faults.

Second, the TI Team modeled the potential for future earthquakes by considering fault sources in terms of single or combined fault ruptures. In this approach, the TI Team considered: (1) rupture of a single fault segment; (2) rupture of two or more adjacent fault segments on the same fault; or (3) rupture of adjacent primary and/or connected fault segments. These ruptures may involve a single sense of slip (e.g., all strike-slip) on all segments or different senses of slip (e.g., reverse and strike-slip) on multiple fault segments. In the SSC SSHAC study (PG&E, 2015e), the TI Team referred to ruptures with single senses of slip as "linked" or "splay," and the ruptures with different senses of slip as "complex." Based on the segments for the four primary faults defined in the fault geometry models and the faulting characteristics of the connected faults, the TI Team then developed a suite of fault rupture sources as a way to capture what they consider to be the full range of possible rupture scenarios. The various combinations of rupture sources with each fault geometry model form what the TI Team referred to as a rupture model; that is, the combinations of all fault segments that can rupture together within a single fault geometry model.

Third, the TI Team assigned slip rates to the various fault rupture models by allocating the available fault slip, which is based on the measured slip rates for the individual faults, among the network of faults described in the fault geometry model. In this approach, the TI Team used the slip rate determined from evidence of fault slip from geological, geophysical, or seismological information as the available slip rate budget, which it then distributed among the various rupture sources. Thus, the slip rate allocation model created a slip rate for each rupture source such that, when the contributions from all rupture sources are summed, the combined slip rate equals the target slip rate budget for that particular fault within that rupture model.

Fourth, the TI Team developed magnitude distribution models for each rupture source to account for the minimum and maximum magnitudes and the relative frequency of earthquake magnitudes over the range from the minimum to the maximum. The TI Team derived the maximum magnitude for each rupture source using the fault-area scaling relationships of Hanks and Bakun (2014). The TI Team also selected four different probability distributions to define the magnitude frequency. For nearly all the single fault segments and shorter linked faults, the TI Team used the characteristic model of Youngs and Coppersmith (1985). For longer linked faults, including faults in which slip occurs on the full length of the Hosgri fault and a significant reach of the San Simeon and San Gregorio faults, the TI Team adopted the WAACY model

(Appendix G of PG&E 2015e). Finally, for complex and splay ruptures, the TI Team used a simple maximum magnitude model (Wesnousky et. al, 1983).

Fifth, the TI Team incorporated time dependency into the SSC model, because they determined that a growing body of seismological evidence shows that earthquake recurrence on many faults is too regular to be considered simply as a time-independent Poisson process (Biasi et al., 2002; Scharer et al., 2010; Fitzenz, 2010). To account for a time-dependent process, the TI Team developed equivalent Poisson ratios and applied those ratios to the primary and connected fault source rates. The methodology for the TI Team's approach is described in Appendix H of the SSC SSHAC report (PG&E, 2015e).

STAFF EVALUATION

The NRC staff reviewed the TI Team's overall approach to developing the SSC model and concludes that the framework established by the TI Team provides a logical and inclusive approach to ensuring that the resulting SSC model captures the center, body, and range of technically-defensible interpretations. Although the TI Team included several new approaches to faulting characterization compared to more traditional SSC models (e.g., Pacific Northwest National Laboratory (PNNL), 2014), the staff determines that the overall SSC model developed by the TI Team contains the essential elements needed to describe the likely future occurrence of earthquakes in the vicinity of the DCPP. These essential elements are: (1) an inventory of all known seismic sources within the vicinity of the DCPP, including both fault and areal sources; (2) characterization of the seismic sources in terms of their size, location, depth, faulting style, and connectivity to other sources, including an accurate assessment of uncertainty; and (3) defensible representations of the location, magnitude, and likelihood of future earthquakes that these seismic sources produce, including an accurate assessment of uncertainty. Discussions of these hazard significant parameters are provided in Sections 3.1.4 and Section 3.1.5 of this staff assessment.

The NRC staff also reviewed the unique approach the TI Team used to develop the rupture models and to allocate the slip rate amongst the rupture sources. The detailed review the TI Team provided on a number of recent historic earthquake ruptures was instructive in pointing out the potential complexities associated with active seismicity in a transpressional tectonic setting. The NRC staff observed that many recent earthquake ruptures reviewed by the TI Team show that these earthquakes ruptured on parallel strands or along connecting faults. The NRC staff concludes that these analogs provide an acceptable technical basis to develop a more realistic representation of fault rupture associated with a fault network similar to that observed at the DCPP site. In particular, the NRC staff concludes that the approach to allocating slip among the seismic sources based on a slip rate budget is acceptable because long-term geologic fault slip rates provide the best available constraint on earthquake recurrence, in the absence of site-specific paleo-earthquake and paleo-seismic data.

Based on review of the technical literature, the NRC staff determines that a slip rate approach is reasonable for seismic hazard analyses in areas without a well-developed earthquake chronology. Finally, the NRC staff concludes that the rupture and slip allocation models developed by the TI Team appropriately capture both the natural variability in how faults deform (i.e., aleatory uncertainty) and the inherent uncertainty in how to represent the fault-deformation

processes in numerical models (i.e., epistemic uncertainty). The NRC staff concludes that the TI Team appropriately captured the uncertainty associated with the application of these faulting models, and that these models are acceptable for use in calculating seismic hazards at the DCPP site.

3.1.4 Fault Sources

As defined in the SSC SSHAC report (PG&E, 2015e), the TI Team identified several categories of fault sources that were considered as part of the SSC. These include four primary faults: Hosgri, Los Osos, Shoreline, and San Luis Bay. These four faults were shown in prior PSHA sensitivity studies (e.g., PG&E, 2011) to contribute significantly to the seismic hazard at the DCPP. The TI Team defined connected faults as faults that are potentially linked to one of the four primary faults and that could have segments that contribute to a single large rupture on a primary fault. In addition to the primary and connected faults, the TI Team also evaluated other regional faults within 320 km of the DCPP. The TI Team organized their fault characterization according to five elements: (1) fault geometry, (2) slip rate, (3) fault rupture, (4) magnitude distribution, and (5) time-dependent models. These five elements are described and evaluated in the next subsections of this staff assessment.

3.1.4.1 Fault Geometry Models

The TI Team developed fault geometry models to describe the location, dip, and physical dimensions of the primary and connected fault sources. The TI Team also used the fault geometry models to capture epistemic uncertainty in the fault sources. The TI Team's motivation for how these fault geometry models was described previously in Section 3.1.3 of this staff assessment. The TI Team also characterized the geometry of other faults within 320 km of the DCPP. For all but five of these regional faults, the TI Team relied on the fault characterization developed in UCERF3 (Field et al., 2013). For the five regional faults sources not included in UCERF3, the TI Team relied on published information to develop simplified fault source characterizations (see Table 12-4 of PG&E, 2015e). Finally, the TI Team included the San Andreas fault, which is located approximately 80 km northeast of the DCPP.

STAFF EVALUATION

The NRC staff reviewed the information in the SSC SSHAC report (PG&E, 2015e) and determined that the TI Team's characterization of the fault geometries of the primary, connected, and regional faults is adequate to develop a technically-defensible PSHA for the DCPP. According to the hazard sensitivity results presented at the first workshop (Wooddell, 2011), other regional faults do not contribute significantly to the DCPP seismic hazard. Based on the same sensitivity analyses, the San Andreas fault also does not contribute significantly to the seismic hazard at the DCPP, except for long period (>1 sec) ground motions. For these reasons, the NRC staff review provided in this staff assessment is only focused on the primary and connected faults that contribute significantly to seismic hazards at the DCPP.

Based on NRC staff's review of the SSC SSHAC report (PG&E, 2015e) and observations at the SSHAC workshops, the NRC staff concludes that the TI Team's fault geometry models for the primary faults were based on an acceptable variety of geological, geophysical, and

seismological information. In particular this information includes significantly detailed seismic imagery of the primary faults in the subsurface, as documented in the CCCSIP Report (PG&E, 2014). The NRC staff notes that the geometric characterization of the Hosgri fault is especially well constrained by the offshore seismic images, in addition to the alignment of relocated hypocenter earthquake data of Hardebeck (Hardebec, 2013).

The NRC staff concludes that the conceptual designs of the fault geometry models are an adequate approach to capturing the center, body, and range of technically defensible interpretations. The NRC staff notes that the three geometry models for the Hosgri fault are straightforward and reasonably capture small differences in the interpreted dip of the fault. In contrast, the NRC staff notes that SLPB fault geometry models are appropriately complex, because these models capture the diverse range in seismotectonic interpretations of the San Luis Range that were presented by the proponents during the second workshop. As described in PG&E (2015e), the TI Team's motivation in developing the fault geometry models, especially the variants for the SLPB faults, was to ensure that the models captured the diverse interpretations among the technical community regarding the nature and style of faults responsible for the uplift of the San Luis Range. The NRC staff also concludes that the approach taken by the TI Team to use these alternative fault geometry models was an effective method to incorporate epistemic uncertainty for these varied seismotectonic interpretations into the PSHA.

In summary, based on the NRC staff's review of SSHAC documentation, observations made at SSHAC workshops, and knowledge of the geological and seismological characteristics of the DCPP region, the NRC staff concludes that the TI Team acceptably implemented a SSHAC Level 3 process to develop the fault geometry models.

3.1.4.2 Fault Slip Rate Models

The TI Team developed slip rates and associated uncertainties for the primary and connected faults that lie within 320 km of the DCPP based on a combination of geological and geophysical data. The emphasis of the TI Team's evaluation was on characterizing the primary faults, especially the Hosgri fault, because the hazard sensitivity analysis presented at the first Workshop by Wooddell (2011) indicated that slip on the Hosgri fault was the dominant contributor to the seismic hazard. To estimate slip rates for the primary faults, the TI Team mainly relied on long-term average slip rates, which were based on observed offsets of geologic markers. Other geological, geophysical, and geodetic data also were used by the TI Team, primarily to check the reasonableness of the estimated slip rates determined from offset geological markers. For these estimates, the TI Team determined total net slip of an offset geologic feature and divided that offset distance by the age range during which that offset occurred, taking into account the geometric corrections needed to account for the sense of slip and dip of the fault plane. To account for uncertainty in the slip rate, the TI Team developed discrete probability distributions for both the age of the offset feature and the amount of fault offset. These probability distributions were triangular (minimum, preferred, and maximum values) or trapezoidal (minimum, range of best estimate, and maximum values). These two discrete probability distributions (age and offset) were then combined by the TI Team using a Monte Carlo method to derive a cumulative slip rate distribution and calculate the mean, median, and other fractile values of slip rate.

Much of the information used by the TI Team to derive the geologic ages of fault slip and associated uplift were derived from the detailed chronology developed by PG&E (2013c). This chronology is based on evidence of the effects of sea level changes on the geologic record that occurred in response to glacial cycles during the last several million years. In essence, sea levels fell and were low during the glacial periods, when much of Earth's water was sequestered in glacial ice. Sea levels rose and were high during periods when the global climate warmed and these glaciers melted. The TI Team relied on this chronology in two ways. First, the TI Team used the relative vertical displacement of paleoshorelines preserved in the Irish Hills to determine uplift rates of the San Luis Range.

Second, the TI Team identified stream channels that were cut into the paleoshorelines during the lowstands (i.e., periods when sea levels were low) and were subsequently buried by sediments and preserved in the offshore sedimentary record during the next highstand (i.e., periods when sea levels were high). The TI Team was able to observe that these paleo-channels were subsequently offset by right-lateral slips on the Hosgri and Shoreline faults, where the paleo-channels crossed these two faults. The amount of offset of these paleo-channels (either best estimate or range of best estimates) was used by the TI Team to quantify the cumulative amount of fault slip since the time when the paleo-channels were first cut into the paleo-shorelines.

The TI Team developed slip rate estimates at four locations along the Hosgri fault trace (see Figure 3.1-3 of this staff assessment). These included: (1) an offset marine terrace strandline near San Simeon (referred to as the Oso Terrace), (2) offset of an approximately 11,500 year old sand spit between Morro Bay and Point San Simeon (referred to as the Cross-Hosgri slope), (3) right-lateral separation of a buried paleo-channel in Estero Bay, and (4) right-lateral separation of a buried paleo-channel near Point Sal. Median slip rates based on these four offset measurements, and ages of the offset features, ranged between 0.8 mm/yr (Point Sal) and 2.5 mm/yr (Cross-Hosgri slope), with a weighted mean from all four sites of 1.7 mm/yr ± 0.7 mm/yr (± 1 standard deviation).

For the Shoreline fault, the TI Team identified three features in San Luis Bay to constrain the slip rate; an offset terrace riser and two apparent offset paleo channels. All three features yield similar median horizontal slip rates of 0.05–0.07 mm/yr. Because all of these offset features are in San Luis Bay south of the Shoreline fault's intersection with the San Luis Bay fault, the TI Team assumed that the Shoreline fault slip adjacent to the DCPP would be slightly larger to account for the small amount of right-lateral slip transferred from the San Luis Bay fault to the Shoreline fault north of this intersection.

For the San Luis Bay and Los Osos faults, the TI Team developed hanging wall and footwall slip rate distributions largely based on the uplift rate of the San Luis Range, which was derived from marine terrace data and from the vertical separation of fluvial deposits observed in paleoseismic trenches (Lettis and Hall, 1994). In addition, the TI Team included new data on localized subsidence in Morro Bay and considered an alternative uplift model based on a newly proposed paleo-sea level model for California terraces (e.g., Muhs et al., 2012). According to PG&E (PG&E, 2015e), these data show that the San Luis Range near the DCPP is uplifting at a rate of between 0.19 ± 0.03 mm/yr and 0.23 ± 0.02 mm/yr (Hanson et al., 1994). Based on these uplift

rates and the alternative interpretation of fault dip (Lettis and Hall, 1994), the TI Team derived the long-term slip rate of the Los Osos fault to be between 0.2–0.7 mm/yr. The San Luis Bay fault was characterized by the TI Team as a reverse fault along the southern margin of the Irish Hills, with a net slip rate of 0.08–0.20 mm/yr, based on a vertical separation rate of 0.07–0.12 mm/yr and a range in fault dip of 40–70 degrees (Lettis and Hall, 1994).

STAFF EVALUATION

The NRC staff reviewed the information provided by PG&E (2015e) and concludes that the TI Team developed an adequate technical basis to determine the fault slip rates of the primary faults. The use of geological markers to establish average slip rates is a well-established method among geologists and seismologists. The NRC staff concludes that this method was used appropriately by the TI Team to develop slip rate estimates for both onshore and offshore faults. In addition, the NRC staff notes that the sensitivity studies conducted for the prior DCPP PSHA (Wooddell, 2011) showed that the most significant contributor to the seismic hazard at the DCPP are the slip rates for the primary faults, especially the slip rate of the Hosgri fault. Based on this sensitivity, the NRC staff's review focused on the slip rate of the Hosgri fault.

For the onshore faults, the NRC staff determined that the slip rates of the San Luis and Los Osos faults were based on the evidence for differential uplift of the Los Osos Range, which was first established during the Long-Term Seismic Program (PG&E, 1991c). These evaluations of the uplifted terraces have undergone significant technical review and reanalysis over the past 25 years, including a detailed evaluation completed by the NRC staff (NRC, 2012c). For this staff assessment, the NRC staff concludes that the TI Team's use of uplift rates for the San Luis Range is sufficient to constrain the slip rates of the SLBP faults. For the offshore faults, the NRC staff determines that the evidence from offset stream channels in the shallow seismic stratigraphy provides a sufficient technical basis to estimate the slip rates for the Hosgri and Shoreline faults. The NRC staff also notes that the estimate of slip rate for the Hosgri fault, which is based on new seismic imaging data, is consistent with prior estimates of the fault slip rate based on other geological data (Hanson et al., 2004).

To confirm the cumulative distributions of fault slips on these primary onshore and offshore faults, the NRC staff recomputed the triangular and trapezoidal distributions for fault slip and age of fault slip based on the data in the SSC SSHAC report (PG&E, 2015e). The NRC staff recombined these distributions using a Monte Carlo method similar to the one relied on by the TI Team. The staff found that the resulting cumulative distributions were consistent with those provided by the TI Team in the SSC SSHAC report (PG&E, 2015e). Based on this independent confirmatory study, the NRC staff concludes that the TI Team adequately determined the statistical range of fault slip rate, which is an important component in fully characterizing the uncertainty associated with the best estimates of fault slip rate.

Because the slip rate on the Hosgri fault is the most significant contributor to the hazard calculation, the NRC staff also conducted an independent confirmatory analysis of fault slip based on the analysis of seismic images of an offshore half-graben (i.e., fault-bound sedimentary basin). This half-graben formed where displacement on the Hosgri fault appears to transfer slip to the San Simeon fault along a right-stepping extensional pull-apart basin. This half-graben and an associated extensional fault zone are situated a few kilometers offshore,

23 km to 40 km northwest of the DCPP. As the pull-apart basin developed, sediments accumulated in the basin, infilling the available accommodation space created by subsidence in the extensional pull apart. Growth of this sedimentary profile within the half-graben is, thus, directly related to slip on the Hosgri fault and the associated opening of its extensional pull-apart basin.

The NRC staff developed an independent estimate of the Hosgri fault slip rate by first measuring the heave (i.e., horizontal component of fault displacement) of the half-graben fault relative to a sediment profile with four age-constrained unconformities, and then relating the growth of this sediment profile to the fault geometry (McGinnis et al., 2016). The NRC staff analyzed these unconformities using seismic sections at 24 locations along the half-graben fault. Based on the geometric constraints of the fault system and the sequence of fault growth, the NRC staff observes that the slip rate on the Hosgri fault appears to increase from a rate of 0.21 mm/yr approximately 2.5 million years ago to a rate of 2.17 mm/yr approximately 20,000 years ago (McGinnis et al., 2016). Considering the analytical uncertainties in this confirmatory analysis, the NRC staff concludes that the youngest (and largest) slip rate is reasonably consistent with the slip rate distribution developed by the TI Team (PG&E, 2015e).

In summary, based on the NRC staff's review of SSHAC documentation, observations made at SSHAC workshops, knowledge of the geological and seismological characteristics of the DCPP region, and independent confirmatory analyses the staff concludes that the TI Team acceptably implemented a SSHAC Level 3 process to develop the fault slip rate distributions for the primary faults near the DCPP site.

3.1.4.3 Fault Rupture Models

The rupture sources in the SSC rupture models are akin to fault sources in a more traditional fault source characterization. For each rupture source, the TI Team determined the size and location of future earthquakes from the geometric properties of that source (i.e., location, length, orientation, and down-dip width). The TI Team assigned a slip rate to each rupture source based on the slip rate of the associated fault. The TI Team also assigned a recurrence model to each rupture source to capture the aleatory variability in the magnitudes and rupture dimensions of possible future earthquakes on the fault. The TI Team noted that the rupture model approach differs from a more traditional PSHA fault characterization in that it accounts for potentially larger and more complex ruptures on a network of linked faults, and thus allows for these larger and more complex ruptures to be included in the SSC model.

STAFF EVALUATION

The NRC staff evaluated the TI Team's use of rupture source models and concludes that these provide a reasonable basis to ensure that the resulting SSC model captures the center, body, and range of technically defensible interpretations. The NRC staff also concludes that the TI Team's approach is an acceptable method to capture the aleatory variability and epistemic uncertainty in fault source characterization. This approach is acceptable because each rupture source accounts for multiple possible future combinations of fault rupture (i.e., aleatory variability) and includes the full distribution of each fault's slip rate. The TI Team's approach accounts for epistemic uncertainty within each rupture source, because alternative slip rates

and associated weights are assigned to each rupture source. Additionally, epistemic uncertainty is captured by the range of fault geometry models used by the TI Team, which represent a reasonable range of alternative interpretations of the seismotectonic setting. Thus, the NRC staff concludes that the TI Team's overall approach and implementation of rupture models are reasonable and adequately capture the center, body, and range of technically defensible interpretations.

In summary, based on the NRC staff's review of SSHAC documentation, observations made at SSHAC workshops, and knowledge of the geological and seismological characteristics of the DCPP region, the staff concludes that the TI Team acceptably implemented a SSHAC Level 3 process to develop the fault rupture models.

3.1.4.4 Magnitude Distribution Models

The TI Team constructed magnitude distribution models to characterize the relative frequency of earthquake magnitudes between the minimum and maximum for each rupture source using four alternative magnitude probability density functions (PDFs). The TI Team used three established and one new alternative magnitude PDFs to develop the magnitude distribution models for future earthquakes. These PDFs are the: (1) truncated exponential (Gutenberg and Richter, 1944), (2) characteristic earthquake (Youngs and Coppersmith, 1985), (3) maximum magnitude (Wesnousky, 1983), and (4) the recently developed Wooddell, Abrahamson, Acevedo-Cabrera, and Youngs (WAACY) model (Wooddell et al., 2014) distributions. The TI Team used either the truncated exponential or the WAACY model for rupture sources greater than 100 km in length with weights of 0.2 and 0.8, respectively. For ruptures less than 100 km, the TI Team used the characteristic earthquake model and distribution for linked ruptures, and the maximum magnitude model for complex and splay ruptures. The TI Team also noted that the resulting magnitude-frequency distributions for the section of each primary fault source closest to the DCPP compared favorably to the magnitude-frequency distributions used by the UCERF3 model.

The TI Team used the Hanks and Bakun (Hanks and Bakun, 2014) magnitude-area scaling relationships to determine the maximum or characteristic magnitudes of each rupture source. To determine the fault rupture area, the TI Team estimated the maximum length of the rupture and also assumed either a 12 km (SLPB) or 15 km (Hosgri) depth to the base of the seismogenic crust. From these estimated maximum rupture areas, the TI Team computed the maximum or characteristic earthquake magnitude. The TI Team initially used multiple magnitude-area scaling relationships but determined that the range of maximum magnitudes produced by the relationships was not significant.

STAFF EVALUATION

The NRC staff evaluated the TI Team's approach to developing magnitude distribution models for each of the rupture sources using four alternative magnitude PDFs and concludes that the approach used by the TI Team is sufficient to ensure that the resulting SSC model captures the center, body, and range of technically defensible interpretations. Specifically, the NRC staff reviewed the information developed by PG&E (2015e) and concludes that the TI Team appropriately used one of the four magnitude PDFs depending on the type of earthquake

rupture. The NRC staff notes that the TI Team used two alternative distributions for the longer (greater than 100 km) ruptures in order to capture the epistemic uncertainty in magnitude distribution for these relatively infrequent events. In addition, the staff notes that the TI Team's decision to more heavily weight the WAACY model is appropriate since the WAACY distribution places higher weight on the larger magnitudes relative to the truncated exponential model. Finally, the NRC staff concludes that the Hanks and Bakun (Hanks and Bakun, 2014) magnitude-area scaling relationships provide an adequate technical basis to develop either the maximum or characteristic earthquake magnitude.

In summary, based on its review and evaluation of applicable information in (PG&E, 2015e), the NRC staff concludes that the TI Team acceptably developed magnitude distribution models for use in the SSC model.

3.1.4.5 Time Dependency Model

In most traditional PSHAs, earthquake recurrence is modeled as a time-independent Poisson process. However, in the SSC SSHAC report (PG&E, 2015e), the TI Team noted that there is emerging consensus among seismologists that fault-specific earthquake recurrence is more uniform than is implied when non-Poisson recurrence is assumed (e.g., Biasi et al., 2002; Scharer et al., 2010; Fitzenz et al., 2010). For a given fault with a characteristic return period, the likelihood of a large, characteristic event is lower in the time interval following a large event and increases through time. To account for potential time dependence, the TI Team implemented an equivalent Poisson ratio (EPR) approach based on recurrence models represented by log-normal, Weibull, and Brownian Passage Time distributions.

Within the TI Team's approach, the EPRs depend on: (1) the long-term mean recurrence rate of moderate to large earthquakes, (2) a coefficient of variation in the model, and (3) the time since the most recent medium- to large- magnitude earthquake. The TI Team derived the mean recurrence rate from the long-term slip rates, as described and reviewed by the NRC staff in Section 3.1.4.2 of this staff assessment. To estimate the time since the last medium to large earthquake, the TI Team relied on two historical observations. According to the TI Team, historical records show that the San Luis Obispo Mission was founded in 1772, and has not experienced any significant earthquake damage since it was built. The TI Team also noted that by the early 1870s, road and rail connections were opened to the rest of California and the first newspaper in San Luis Obispo was established. Based on these observations, the TI Team set the minimum time since the last medium- to large- magnitude earthquake at 140–242 years. Considering this range in time since the last earthquake, the calculated recurrence interval for the Hosgri and SLPB faults, and a range of coefficients of variations based on values for best available paleoseismic records in California, the TI Team determined an average EPR of 1.3 for the Hosgri fault and an average EPR of 1.1 for the SLPB faults. These average EPRs and associated distributions were implemented in the SSC logic tree as the first nodes for these faults.

STAFF EVALUATION

The NRC staff reviewed the information in the SSC (PG&E, 2015e) and determined that the TI Team developed an adequate technical basis to incorporate a fault-specific, time-dependent

model into the PSHA. The TI Team's approach appropriately reflects the emerging consensus among the seismological community that these time-dependent models are necessary to capture the center, body, and range of technically-defensible interpretations. Because of the lack of paleoseismic information to constrain the age of past earthquakes on the Hosgri or SLPB faults, the NRC staff also concludes that the TI Team's use of historical observations is acceptable. As noted by the TI Team, the 140–242 years since the last damaging earthquake are minimum values, based on the lack of recorded earthquakes in the local historical record. Moreover, based on the formulation developed by the TI Team, as the time since the last earthquake is increased, the EPRs for the Hosgri and SLBP faults get smaller. Thus, the 140–242 year values used by the TI Team are deemed by the NRC staff to be conservative. The NRC staff also concludes that the coefficient of variation determined from best available paleoseismic records in California is adequate because this value should represent the average value of fault behavior and these records provide a reasonable record of that behavior. Finally, to further evaluate the acceptability of using the time-dependent approach within the PSHA, the NRC staff performed a confirmatory evaluation in which the NRC staff was able to reproduce the TI Team's EPR results.

In summary, based on the NRC staff's review of SSHAC documentation, observations made at SSHAC workshops, and a confirmatory calculation, the staff concludes that the TI Team acceptably accounted for a time-dependent Poisson process in the SSC model.

3.1.5 Areal Source Zones

In addition to the fault sources (see Section 3.1.4 of this staff assessment), the SSC model developed by the TI Team accounted for potential seismicity occurring from other faults within 320 km of the DCPP site through the use of areal source zones. Areal sources include less active and less well-defined geologic fault zones, which the TI Team characterized with a defined location, crustal thickness, earthquake recurrence parameters, maximum magnitude, and magnitude frequency distribution shape. The areal source zones contain faults that are known, proposed, or unknown. However, these faults have insufficient data for modeling, and they are not sufficiently active or well-constrained to be considered as separate fault sources.

As described in Chapter 13 of the SSC (PG&E, 2015e), the TI Team developed three non-overlapping, nested areal sources zones: Regional, Vicinity, and Local. Because past hazard sensitivity analyses showed that hazard at the DCPP is dominated by ground motions caused by earthquakes occurring at close distances on the primary fault sources (PG&E, 2011; Wooddell, 2011), the TI Team used simplified approaches for modeling the areal source zones that included an increasing level of detail closer to the DCPP. The Regional and Vicinity areal source zones correspond approximately to the Site Region (i.e., 320 km) and Site Vicinity (i.e., 40 km) zones, as defined in Regulatory Guide 1.208 (NRC, 2007). The TI Team modeled the occurrence of potential earthquakes in the Regional and Vicinity areal source zones as point sources. For the Local areal source zone, the TI Team modeled earthquakes as occurring on a set of parallel virtual faults.

To develop distributions of the size and frequency of earthquakes in all three areal source zones, the TI Team evaluated the occurrence of past earthquakes from four earthquake catalogs: (1) a 2014 non-declustered relocated earthquake catalog (see Appendix F; PG&E,

2015e); (2) a declustered catalog developed by PG&E's Geosciences Department (see Appendix F; PG&E, 2015e) with converted moment magnitude rates; (3) the updated UCERF3 catalog (declustered); and (4) a compilation of historical earthquakes by McLaren and Savage (2001). In addition, the TI Team used the truncated exponential (Gutenberg and Richter, 1944) magnitude frequency distribution to define the recurrence relationships for future earthquakes with *a*- and *b*-value determined from the seismicity rates indicated by the four earthquake catalogs.

The TI Team used the gridded seismicity file developed as part of UCERF2 (Petersen et al., 2008) as a baseline model for the areal source zones in the SSC model. For the Regional and Vicinity areal source zones, the TI Team modeled earthquakes as a set of point sources on regularly spaced grids and applied distance adjustments. The TI Team justified use of this approach due to the greater distances from the DCPP site where less precision in earthquake location was needed, compared to the Local source zone. The rates of earthquakes in the gridded source zones were calculated based on observed and spatially smoothed seismicity rates and model predictions about M_{max}. For the Regional areal source zone, which is the zone furthest from the DCPP, the TI Team did not make any rate adjustments to the baseline model. For the Vicinity model, the TI Team incorporated epistemic uncertainty by scaling the seismicity rate in the baseline model based on comparison to observed rates in the earthquake catalogs.

For the Regional and Vicinity source zones, the TI Team used spatially smoothed seismicity grids to represent the spatial density of earthquake occurrences and the distribution of future earthquake recurrence. The TI team modeled M_{max} for the Regional and Vicinity source zones following the UCERF3 approach for maximum off-fault magnitude (Field et al., 2013). To model the style of faulting, the TI Team included 70 percent strike-slip and 30 percent reverse-slip earthquakes, based on the relative rate of these earthquakes in the catalogs and the dominantly transpressional environment of the DCPP site.

For the Local areal source zone, the TI Team modeled 18 subparallel, 50-km-long faults striking N50°W, with a spacing of 1 km (see Figure 3.3-1 of this staff assessment). The TI Team modeled the characteristics of these virtual faults by their fault geometry (i.e., location, strike, length, down-dip width, and dip), sense of slip, and M_{max}, including both aleatory and epistemic uncertainty. The TI team developed these characteristics from geologic, geophysical, and seismological data, such that the resulting virtual faults are consistent with its interpretations of the overall geologic structural and seismotectonic setting of the DCPP site. The sense of slip information was derived by the TI Team from the single-event and composite focal mechanisms from Hardebeck (2010, 2014), with additional data and analysis presented at the SSHAC workshops. The TI Team determined the rates of earthquakes in this areal source zone based on observed seismicity rates and considerations of geologic rates of deformation. Similar to the Regional and Vicinity source zones, the TI Team distributed the seismicity as 70 percent strike-slip and 30 percent reverse-slip earthquakes. The TI Team estimated M_{max} on the virtual faults based on the maximum dimensions of the virtual faults and applying the same magnitude-area scaling relationships used for the primary and connected fault sources.

STAFF EVALUATION

Based on its review of the information in the SSC SSHAC report (PG&E, 2015e), the NRC staff concludes that the TI Team adequately accounted for the potential seismic hazard from unrecognized faults through its development of the three areal source zones in the SSC model. The staff also concludes that the TI Team adequately characterized the uncertainty in the location, magnitude, and recurrence rate of potential earthquakes within the areal source zones by using a combination of spatially smoothed point sources for the two distant areal source zones, and virtual faults for the Local areal source zone. The size and location of the three areal source zones is deemed acceptable by the NRC staff, because the TI Team's approach is consistent with the guidance in Regulatory Guide 1.208 (NRC, 2007).

The NRC staff concludes that the TI Team developed an acceptable record of past earthquake information for the areal source zones, as contained within the four earthquake catalogs. These catalogs have undergone extensive evaluation and review by the several government agencies, including the USGS and the California Geological Survey. As described in Appendix F of PG&E (2015e), earthquakes included in these catalogs come from two well-established seismic networks: the California Integrated Seismic Network (CISN), which is operated by the USGS, Caltech, and the University of California at Berkeley, and the Central California Seismic Network, which is operated by PG&E. In addition, many of the earthquake hypocenters in these catalogs were relocated using one of two double difference codes; the double difference tomography program of Zhang and Thurber (2003) or the HypoDD code of Waldhauser and Ellsworth (2000). The NRC staff notes that these relocations significantly improve the spatial resolution of the hypocenter data and increase the confidence in associating these earthquakes with mapped faults. The detailed development and ongoing maintenance of these earthquake catalogs provides the NRC staff with assurance that these data are sufficiently reliable to allow the TI Team to develop an acceptably accurate model of the areal source zone seismicity, which captures the center, body, and range of the technically defensible interpretations.

In addition, the NRC staff concludes that the TI Team developed technically-defensible representations of M_{max} and the frequency of earthquake recurrence. The NRC staff notes that the use of the truncated exponential (Gutenberg and Richter, 1944) magnitude frequency distribution to define the recurrence relationships for future earthquakes is a standard approach that has been successfully applied to the characterization of areal source zones across the U.S., including the recent SSC model for the CEUS (NRC, 2012b). In addition, the NRC staff concludes that the values of M_{max} in the SSC model are acceptable because they are based on the generally accepted UCERF3 model of maximum off-fault magnitude (Field et al., 2013), as well as a realistic consideration of the potential rupture areas of the virtual faults given the range of fault geometries in the region and the 12–15 km depth of the seismogenic crust.

Finally, the NRC staff concludes that the TI Team acceptably used and characterized the virtual faults to model the future occurrence of earthquakes inside the Local areal source zone. The NRC staff notes that this approach provides a more realistic representation of the location and distribution of future earthquakes, because it accounts for the geological and seismotectonic characteristics of the seismic sources. In addition, this approach treats the occurrence of future earthquakes as actual fault plane ruptures rather than point sources. The NRC staff also concludes that the geometric characteristics of the virtual faults are reasonably representative of

the nature and styles of the local and regional faults, because they are consistent with the primary and connected fault zones that are described and reviewed in Section 3.1.4 of this staff assessment. Further, the characteristics adopted are consistent with the observed focal mechanisms and micro-seismicity trends described in Hardebeck (2014). Finally, based on the confirmatory calculations performed by the NRC staff and documented in the Section 3.3.2 of this staff assessment, the NRC staff concludes that the contribution of the Local areal source zones to the seismic hazard at the DCPP were acceptably accounted for in the DCPP PSHA.

In summary, based on its review and evaluation of applicable information provided by PG&E (2015e), the NRC staff concludes that the TI Team acceptably developed areal source zones for use in the SSC model.

3.2 Ground Motion Characterization

The two GMC models for the DCPP PSHA, developed by the TI Team as part of the SWUS SSHAC Level 3 GMC (GeoPentech, 2015), characterize median ground motions and their associated aleatory variability (i.e., sigma): one for nearby and one for distant earthquakes. Specifically, the GMC models consist of two suites of ground motion prediction equations (GMPEs) for five percent damped horizontal spectral accelerations at 17 spectral periods between 0.01 and 10 seconds. To capture the epistemic uncertainty in both the predicted median ground motions and the aleatory variability, the TI Team developed logic trees with each branch on the tree representing an individual GMPE with an assigned weight. The GMPEs developed by the TI Team assume WUS reference baserock site conditions. The licensee subsequently adapted these median GMPEs to account for site-specific conditions at the DCPP.

3.2.1 Assessment of the SSHAC Process for GMC

To develop the GMC models, the TI Team implemented the SSHAC Level 3 process by first evaluating available data, methods, and models of relevance to the characterization of ground shaking at the DCPP site. The TI Team then used its evaluation of these data and models to construct logic trees for the median ground motions and their associated aleatory variability for the GMC models.

For the SWUS SSHAC Level 3 study, the GMC TI Team conducted three formal workshops and multiple working meetings over a three-year time period from 2012 to 2014. During the first workshop (held March 19–21, 2013), the TI Team identified the ground motion issues of highest significance for the DCPP PSHA and resource experts described the available ground motion databases and models. In particular, the TI Team discussed the need to use ground motions developed from numerical simulations in order to evaluate current GMPEs. During the second workshop (held October 22–24, 2013), several proponent experts presented their viewpoints regarding the GMPEs under consideration for the GMC. In addition, participants of the second workshop discussed the need for special consideration of near-field long-period ground motions from larger earthquakes (>**M**7.0). During the third workshop (held March 10–12, 2014), the TI Team described its preliminary GMC models and hazard sensitivity analyses in order to get feedback from the PPRP. Specifically, the TI Team provided a more detailed description of the Sammon's map approach (see Section 3.2.3.1 of this staff assessment), discussed alternative

modeling approaches for complex earthquake rupture scenarios, and discussed the use of alternative distributions for the ground motion residuals.

After the third workshop, the TI Team continued to refine the GMC model and interact with the PPRP. After reviewing the preliminary SSHAC report, the PPRP provided extensive comments to the TI Team and then reviewed the TI Team's responses. In summary, the PPRP concluded in its endorsement letter (GeoPentech, 2015):

> As summarized in the table above, the PPRP reviewed the TI Team's evaluations of data, models and methods on multiple occasions, and through various means, including written communications, in-person meetings, teleconferences, and review of the project report. The Panel was given adequate opportunity to question the TI Team concerning details of their analysis, and provided feedback verbally and in writing. The TI Team was responsive to the technical input from the Panel. The TI Team's responses included evaluating additional data sets suggested by the Panel, undertaking additional analyses to address specific Panel technical questions, and examining and assessing alternative technical approaches suggested by the Panel.
>
> The PPRP therefore concludes that it has been afforded an adequate basis for technical assessment of the TI Team's evaluations and model integration and finds that the project meets the technical expectations for a SSHAC Level 3 study.

STAFF EVALUATION

Based on observations at the workshops and review of the workshop proceedings, the NRC staff concludes that the SSHAC workshops were conducted in a manner consistent with applicable NRC guidance. In addition, the NRC staff did not find significant departures from the guidance in the approach used by the TI Team to develop the GMC models. At the workshops, the staff observed that the TI Team invited and engaged with resource and proponent experts that represented a wide variety of scientific viewpoints. Based on this information, the staff concludes that the TI Team was able to focus its data collection and analysis activities in order to develop GMC models tailored specifically to the types of earthquakes that dominate the hazard for the DCPP site.

An important component of the SSHAC process is complete documentation. Based on its review, the NRC staff concludes that the SSHAC documentation (GeoPentech, 2015) provides an acceptably complete record of the approach used to develop the GMC model.

To evaluate the effectiveness of the PPRP for the GMC model development, the NRC staff examined the PPRP and TI Team correspondence, including the comment and response logs and the letters exchanged following each of the workshops. The staff also observed the open dialog between the TI Team and PPRP at each of the workshops, which included several significant comments from the PPRP that required appreciable effort from the TI Team to resolve. Based on its observations, the staff concludes that the PPRP actively participated in the workshops and provided an extensive and comprehensive review of the GMC models and

PSHA report. In summary, the NRC staff concludes that the PPRP was effective and engaged throughout the SSHAC Level 3 PSHA, and that there were no unresolved PPRP issues at the end of the project.

In summary, based on its review of the SSHAC documentation, observations made at the SSHAC workshops, and knowledge of GMPEs used for active tectonic regions, the NRC staff concludes that the SWUS SSHAC Level 3 study acceptably implemented the SSHAC Level 3 process.

3.2.2 Ground Motion Databases and Seed Model Selection

To develop the two GMC models, the TI Team evaluated a suite of data and models relevant to the hazard for the DCPP site. In particular, the TI Team evaluated recently developed GMPEs for shallow crustal earthquakes in active tectonic regions and regional data to assess the applicability of the GMPEs. The TI Team also created a finite-fault simulation data set to augment the regional data set. To evaluate the available GMPEs for use as inputs to the two GMC models, the TI Team developed a set of objective criteria based on its assessment of best practices in ground motion modeling and also considered the predominant earthquake source mechanisms for the region surrounding the DCPP site.

The TI Team used the Pacific Earthquake Engineering Research (PEER) Next Generation Attenuation (NGA)-West2 database (Ancheta et al., 2014) and a database of ground motions from finite-fault simulations (Maechling et al., 2015) to evaluate the existing GMPE models relevant to the DCPP site and to develop new GMPE models. The NGA-West2 database includes worldwide ground motion data recorded from shallow crustal earthquakes in active tectonic regions. To develop a dataset to evaluate the GMPEs for the local earthquake sources, the TI Team focused its selection on earthquakes with >**M**5 that were recorded at multiple stations (more than three recordings) within 70 km (R < 70km) of the epicenter. In addition, each of the recording sites has a V_{S30} (i.e., travel-time-averaged shear wave velocity in the top 30 m) greater than 250 m/s. The resulting database of earthquake recordings consists of about 200 earthquakes with at least one recording. To supplement this database, the TI Team developed a database of ground motions from finite-fault simulations. The scenarios selected by the TI Team for the simulations include: (1) near-fault ground motions from larger earthquakes (>**M**7); (2) ground motions from complex ruptures (.e., single rupture on multiple faults with more than one sense of slip on adjacent fault sections); and (3) ground motions from splay ruptures (i.e., a rupture source that includes overlapping faults that rupture simultaneously).

In additional to gathering and evaluating ground motion databases, the TI Team also evaluated 19 recently developed and published GMPEs for shallow crustal earthquakes in active tectonic regions. Important criteria developed by the TI Team for the selection of candidate GMPEs include:

- Selection of the most recently published GMPEs over earlier versions,
- Selection of GMPEs suitable for large magnitudes and distance ranges,

- Exclusion of GMPEs developed only for small specific regions,
- Exclusion of GMPEs that have not been peer reviewed or vetted by the larger scientific community, and
- Exclusion of GMPEs developed as research tools rather than for engineering applications.

Based on these criteria, the TI Team selected all five of the NGA-West2 GMPEs (Abrahamson et al., 2014; Boore et al., 2014; Campbell and Bozorgnia, 2014; Chiou and Youngs, 2014; and Idriss, 2014) for use as seed models for characterizing the hazard for both the local and distant sources. For the local sources surrounding the site, the TI Team included three additional GMPEs (Akkar et al., 2014; Zhao et al., 2006; Zhao and Lu, 2011) as seed models.

STAFF EVALUATION

Based on observations at the SSHAC workshops, review of the SSHAC report and knowledge of current GMPEs developed for active tectonic regions, the NRC staff concludes that the TI Team developed an appropriate set of ground motion databases and gathered and evaluated a suitable range of candidate GMPEs. During the first workshop, the staff observed that the TI Team described the available databases in detail and appropriately considered input from the PPRP in selecting the final databases and developing the criteria for evaluating the candidate GMPEs. The staff notes that the PEER NGA-West2 ground motion database consists of several thousand earthquake records and covers a wide range of magnitudes and distances. The staff finds that the TI Team appropriately selected >**M**5 earthquakes recorded at distance within 70 km, from which the TI Team developed a database for the evaluation of the GMPEs for the local sources. In addition, the staff concludes that the TI Team appropriately augmented this local database with near-field ground motions from larger earthquake (>**M**7) simulations.

The NRC staff used its experience in developing and evaluating GMPEs to determine that the TI Team selected an appropriate set of initial candidate GMPEs and used appropriate criteria to select the final set of input GMPEs. Specifically, the staff notes that the criteria used by the TI Team resulted in a set of input GMPEs that have been formally peer reviewed, developed specifically from shallow crustal earthquakes in active tectonic regions, and that are the latest versions of the developers published GMPEs.

In summary, the NRC staff concludes that the TI Team developed suitable ground motion databases and selected an appropriate set of input GMPEs consistent with the fundamental goal of the SSHAC process to objectively evaluate and examine available data and a diverse range of candidate models.

3.2.3 Median Ground Motions

The two GMC models developed by the TI Team for the DCPP PSHA consist of two sets of median GMPEs for local and distant fault sources. Each GMPE predicts median spectral accelerations in terms of magnitude, various source-to-site distance measures, depth to the top of rupture, and fault dip angle, and fault type (i.e., strike-slip, normal, or reverse). For the

nearby fault sources, as well as the Local source zone, the TI Team developed a set of GMPEs by implementing a two-dimensional visualization process, commonly referred to as Sammon's maps (Sammon, 1969). The purpose of the Sammon's map approach is to develop a continuous distribution of median GMPEs that also captures alternative magnitude- and distance-scaling approaches. The GMPEs developed by the TI Team for the local sources also explicitly account for potential hanging-wall effects (i.e., increases in ground motion at short distances for sites on the hanging-wall side of the rupture). For the distant fault sources, such as the San Andreas fault, the TI Team simply used the five GMPEs developed by the NGA-West2 project (Bozorgnia et al., 2014) with additional epistemic uncertainty to capture the potential range of motions from larger magnitude (>**M**7) earthquakes.

3.2.3.1 Median Models for Local Sources

The objective of the TI Team for the SWUS project was to capture the center, body, and range of the continuum of ground motion space (i.e., the full range of median ground motions estimated over a broad range of magnitudes and distances). Rather than merely attaching weights to existing discrete GMPEs, the TI Team developed a suite of GMPEs that was not limited to existing GMPEs and that fully spans and efficiently samples the range of ground motion space. The TI Team recognized that the characterization and quantification of uncertainties, in particular epistemic uncertainties, is a fundamentally important element of the GMC activity. Previous practice has often consisted of representing the epistemic uncertainty in GMC through weighted branches on a logic tree, where the branches represent existing GMPEs. To develop the suite of GMPEs for the SWUS project, the TI Team followed a multi-step process that included utilization of higher-dimensional visualization tools. The steps of this process are summarized below.

First, the TI Team compiled a selection of current, well-documented candidate GMPEs and defined a subset of the candidate models based on technical defensibility and applicability for use in the DCPP region (as described in Section 3.2.2 of this staff assessment). These models were used as seed models as the initial step in the process to develop a comprehensive suite of GMPEs for the local DCPP sources. Based on an evaluation of the characteristics of the candidate seed models, the TI Team identified a common functional form for the development of new GMPEs. This common functional form is parameterized in terms of magnitude, distance, and style of faulting, and contains eleven coefficients.

Next, the TI Team assessed prior PSHA results for the DCPP site (PG&E, 2011) to determine a hazard-informed range of magnitudes and distances to be used in the development of the final suite of GMPEs. The TI Team exercised each of the eight seed GMPEs over the appropriate range of magnitudes (**M**5 to **M**7.5) and distances (up to 80 km). The common form model was then fit to the spectral acceleration results from each of the seed GMPEs, resulting in eight common-form model versions that represent the original seed models. Based on the fitted values of each of the eleven coefficients in the common form models, the TI Team calculated the mean and variance for each of the coefficients, as well as the covariance among the coefficients. Using the common form model, the mean, and the covariance structure of the coefficients, the team developed a suite of 2,000 totally new candidate GMPEs that span the ground motion space.

Although the resulting suite of 2,000 GMPEs spans the ground motion space, this large number of models is computationally impractical for use in a PSHA. Thus, the TI Team used high-dimensional visualization tools to discretize this space into a manageable number of models for the GMC. Specifically, the TI Team exercised the 2,000 GMPEs over a specified set of magnitude and distance pairs. For each GMPE, the ground motion values over this set of magnitude and distance pairs was represented by a high-dimensional vector. The TI Team then utilized principal component analysis and Sammon's mapping (Sammon, 1969) to project each of the high-dimensional ground motion vectors as a point on a two-dimensional Sammon's map.

Based on an analysis of the projected candidate GMPEs and scaled versions of the seed GMPEs, the TI Team identified a range of plausible ground motion space on the Sammon's map, which the team represented as an ellipse. The TI Team subdivided the ellipse into 31 discrete cells and specified a single representative GMPE for each cell. Using several metrics based on consistency with data (i.e., the NGA-West2 DCPP dataset) and the distribution characteristics of the common form models within each cell, the TI Team determined weights for each of the 31 GMPEs. The criteria the TI Team used resulted in a broad range of weighted GMPEs, with some receiving a weight of zero. The TI Team repeated this process for each of the spectral periods.

3.2.3.2 Median Models for Distant Sources

To develop the GMC model for the distant sources (i.e., all sources other than the local faults), the TI Team selected the five NGA-West2 GMPEs, and then added three branches to the logic tree to account for additional epistemic uncertainty in ground motions from larger magnitude (>**M**7) earthquakes. Even though these fault sources (e.g., the San Andreas fault) are capable of generating large-magnitude earthquakes, because of their distance from the site, the TI Team determined that they contribute less than a few percent at the 10^{-4} annual exceedance frequency to the long-period hazard (i.e., less than about 1 second) at DCPP. As such, the TI Team decided that the Sammon's map procedure was not needed to represent the hazard from distant sources, and instead simply assigned equal weights to the five NGA-West2 GMPEs.

STAFF EVALUATION OF MEDIAN MODELS FOR LOCAL AND DISTANT SOURCES

Based on review of the SSHAC documentation and knowledge of current GMPEs developed for active tectonic regions, the NRC staff concludes that the two GMC models developed by the SWUS TI Team provide an appropriate set of GMPEs in order to characterize the hazard for the DCPP site. The staff notes that the TI Team appropriately expanded the initial set of seed GMPEs to develop two larger sets of GMPEs for the local sources and the distant regional sources.

The staff finds that the Sammon's mapping approach used by the TI Team was appropriately applied for the local sources to address the large range of epistemic uncertainty associated with modeling near-site earthquakes. The staff also finds that a more traditional, weighted-GMPE approach was appropriately used for the distant earthquakes, where sufficient data exists to model these types of events, which have minimal impact on the hazard. Therefore, the staff concludes that these two approaches, although dissimilar, are reasonable as applied to the two distinct source types (i.e., local sources and distant regional sources). This is because both

approaches produce a broad suite of median models, each of which are appropriately adapted for the particular source types. The staff finds that these two approaches reasonably account for the epistemic uncertainty in the median ground motions for both local and distant sources.

To evaluate the distribution of median GMPEs produced by the TI Team for the local sources, the NRC staff examined the behavior of the models for multiple earthquake magnitude and source-to-site distance combinations. Figure 3.2-1(a-b) of this staff assessment shows the distribution of weighted medians produced by the set of GMPEs using the Sammon's map approach for the local sources. Specifically, Figure 3.2-1(a) shows the distribution of weighted median results from the 22 GMPEs developed for a spectral period of 0.1 s for a **M**6.5 earthquake for source-to-site distances ranging from 1 km to 100 km. Similarly, Figure 3.2-1(b) shows the same GMPEs for a source-to-site distance of 15 km for earthquake magnitudes ranging from **M**5 to **M**9. Shown in the inset to Figure 3.2-1(a) is the weighted distribution of median spectral accelerations for a **M**6.5 earthquake at a source-to-site distance of 15 km. As shown by the inset to Figure 3.2-1(a), the 22 predicted weighted medians are centered at a reasonable value (0.4g) and cover a suitably wide range of spectral accelerations (0.2g to 0.6g). In addition, Figures 3.2-1(a) and (b) show that the 22 median GMPEs have alternative magnitude and distance scaling approaches, as demonstrated by the intersecting models.

In summary, as a result of this review, the NRC staff concludes that the two sets of GMPEs developed by the TI Team have been appropriately adapted for the seismic sources surrounding DCPP and, as a result, are suitable for use in the PSHA. The staff further concludes that the high-dimensional visualization and sampling through application of Sammon's mapping used by the TI Team for the local sources as well as the traditional approach used for the distant sources are consistent with the intent of the SSHAC guidelines of developing models that capture the center, body, and range of the technically-defensible interpretations of available data, models, and methods.

3.2.4 Ground Motion Variability

In addition to developing GMPEs that predict median ground motions, the TI Team developed models to characterize the random (i.e., aleatory) variability about the median ground motions. To develop these models, the TI Team used the ground motion databases and backbone GMPEs described in Sections 3.2.2 and 3.2.3 of this staff assessment. Because Enclosure 1 to the 50.54(f) letter (NRC, 2012a) requests that licensees perform a detailed site response analysis, the TI Team first separated the residuals between the predicted and observed ground motions into their component pieces in order to remove the repeatable effects of site response. The TI Team then combined the standard deviations for each of the remaining components of the total residuals to produce the total aleatory standard deviation, which is referred to as "single-station sigma" and denoted by σ_{SS}. In order to use the single-station sigma approach, the TI Team captured the site-specific portion of the uncertainty by developing: (1) a set of site terms, (2) distributions for the local site response amplification factor, and (3) a distribution for the epistemic uncertainty of σ_{SS}. The staff's review of the site term and amplification factors is provided in Section 3.4 of this staff assessment.

The single-station sigma approach starts with separating the total residuals into between-event and within-event residual components, where the between-event and the within-event residuals

have standard deviations, referred to as τ and φ, respectively. The within-event residual is then further separated into a site-term component and a site- and event-corrected residual component with standard deviations, referred to as φ_{S2S} and φ_{SS}, respectively. The single-station sigma approach then excludes the site term standard deviation (φ_{S2S}) from the total sigma and instead evaluates φ_{S2S} as epistemic uncertainty.

To develop a model for single-station sigma (σ_{SS}) for the crustal earthquake GMPEs, the TI Team first constructed models for the between-event standard deviation τ and the single-site within-event standard deviation φ_{SS}, assuming both models depend on earthquake magnitude. The TI Team developed a model for τ by averaging the τ models from four of the five NGA-West2 GMPEs along with the Zhao et al. (2006) model. For the φ_{SS} model, the TI Team used the NGA-West2 dataset along with the Taiwanese data from Lin et al. (2011). The TI Team further partitioned the NGA-West2 dataset into a California-only subset, giving this subset a higher weight (0.67) compared to the weight (0.33) for the entire NGA-West2 dataset.

In addition to developing models for each of the individual components of sigma (τ and φ_{SS}), the TI Team developed epistemic uncertainty distributions for each of these components. The TI Team next combined these epistemic uncertainty distributions to develop a final continuous distribution for σ_{SS}, which it represented by three discrete points selected at the 5th, 50th, and 95th percentiles (low, central, and high values).

STAFF EVALUATION

Based on review of the SSHAC report and knowledge of current GMPEs developed for active tectonic regions, the NRC staff concludes that the TI Team developed an appropriate set of models for the ground motion variability in order to capture the full distribution of ground motions generated by the multiple sources in the DCPP SSC model. The staff finds that the TI Team appropriately separated the individual components of the residuals in order to extract the site term, which it estimated using strong-motion records recorded at the DCPP. The staff also concludes that the TI Team used reasonable approaches to model the standard deviations for the individual components of the total variability for the single-station sigma approach.

The NRC staff notes that the ground motion data sets, described in Section 3.2.2 of this staff assessment, contain thousands of earthquakes, many of which are recorded at multiple sites. The NRC staff also notes that the TI Team appropriately developed a California-only subset of the NGA-West2 ground motion dataset to develop a φ_{SS} model. In addition, the staff concludes that the TI Team used an appropriate approach to combine the standard deviations for the individual components of the residuals into a final distribution for σ_{SS} and that this distribution is adequately represented by including three branches in the logic tree.

To evaluate the ground motion variability about the predicted median spectral accelerations, the NRC staff compared the values predicted by the TI Team's τ and φ_{SS} models with estimates calculated from other GMPEs. Based on these comparisons, the staff concludes that the TI Team's τ and φ_{SS} models, as well as the resulting single-station sigma model, produce reasonable estimates of the ground motion variability for each of the earthquake scenarios considered for the DCPP PSHA. Figure 3.2-2, which displays the low, central, and high values for the three components of aleatory variability (τ, φ_{SS}, σ_{SS}) as a function of magnitude, shows

that the values of σ_{SS}, which are used directly in the PSHA calculations, reasonably vary from about 0.6 to 0.5 for earthquake magnitudes ranging from **M**5 to **M**9.

The staff notes that for each local earthquake scenario, the GMC model consists of 20 to 30 alternative median predictions, which after combining with the three alternative sigma values, results in a total of 60 to 90 alternative ground motion distributions. Similarly, for each distant earthquake scenario, there are 15 or 45 alternative ground motion distributions, depending on the magnitude of the earthquake. The staff finds that the TI Team's use of this large number of distributions for each of the earthquake scenarios considered in the DCPP PSHA adequately captures the epistemic and aleatory uncertainty in predicted ground motions for the baserock conditions at the DCPP site.

As a result of this review, the NRC staff concludes that the TI Team appropriately modeled the aleatory variability in ground motions for the DCPP PSHA. Based on this conclusion, the staff finds that the resulting models adequately capture the center, body, and range of technically defensible interpretations.

3.3 Probabilistic Seismic Hazard Analysis

The licensee implemented the SSC and GMC models to develop baserock PSHA hazard curves for the DCPP site. For the GMC model, the TI Team selected the reference baserock condition to be a soft rock with a V_{S30} value of 760 m/s. In accordance with the guidance specified in the SPID (EPRI, 2012), the licensee used a minimum **M**5.0 earthquake and included all seismic sources within 320 km of the site for the DCPP PSHA. The licensee developed individual PSHA hazard curves for each of the seismic sources and observed that only the sources within 15 km of the DCPP contribute significantly (at least 5 percent) to the total hazard at annual frequencies of exceedance of 10^{-3} or smaller.

Summary of PSHA Implementation and Results

For the SSC model, the TI Team characterized the local Hosgri, Shoreline, Los Osos, and San Luis Bay faults as primary fault sources that could potentially rupture along with adjacent or connected faults. In contrast with previous PSHAs for DCPP, the TI Team modeled several rupture combinations between the primary and connected fault sources within each of four alternative tectonic models (Hosgri, Outward Vergent, Southwest Vergent, and Northeast Vergent). These models represent alternatives in tectonic interpretations and fault source characterizations. The SSC logic tree developed by the TI Team for the primary and connected fault sources also captures alternative fault time-dependent parameters, fault geometry models, rupture models, maximum magnitudes, magnitude density functions, and the slip rate allocations for each of the rupture models. Each of these alternatives or characteristics is represented as a node in the SSC logic tree with multiple weighted branches at each node.

The TI Team developed a logic tree for each of the three areal source zones (Local, Vicinity, and Regional), which characterize potential earthquake sources whose general geometry and sense of slip are known, but are not sufficiently active or well-constrained to be considered as separate sources. The logic tree for each of the areal sources defines a unique set of parameters for future potential earthquakes, primarily based on the characteristics of known

Quaternary faults and historical seismicity within each of the source zones. To represent earthquake occurrences within the Local source zone, the TI Team constructed a set of virtual faults. The TI Team included epistemic uncertainties for the location, sense of slip, dip, and maximum magnitude for the virtual faults. For the more distant Vicinity and Regional area sources, the TI Team used a grid of point source approximations rather than virtual faults.

In addition to characterizing the local fault sources and areal source zones, the TI Team also characterized several regional fault sources based on the UCERF3 model (Field et al, 2013). Amongst the regional fault sources, the San Andreas fault, located approximately 80 km northeast of DCPP, moderately contributes to the total hazard for the DCPP. The other regional fault sources contribute less than 1 percent to the total hazard for the DCPP.

The SWUS GMC TI Team developed logic trees for the median and sigma models for both the local and regional earthquake sources. The GMC logic tree for the local earthquake sources includes multiple branches for each alternative GMPE, developed by the TI Team through implementation of the Sammon's map approach. In addition to the logic tree branches for each of the GMPEs, the TI Team included five branches to characterize alternative hanging-wall effects (i.e., increases in ground motion at short distances for sites on the hanging wall side of the rupture). The single-station sigma logic trees include nodes and branches for low, central, and high values as well as the use of either a normal distribution or a mixture model for the final distribution of ground motion residuals.

After implementing the SSC and GMC models for the DCPP PSHA, the licensee developed baserock hazard curves for each of the major fault and areal sources. For both the 1 and 10 Hz spectral acceleration hazard curves, the licensee determined that the hazard from the Hosgri Fault contributes most to the total hazard. In addition to developing hazard curves for each of the seismic sources, the licensee performed a deaggregation of the hazard for both 1 and 10 Hz spectral accelerations at 10^{-4} and 10^{-5} mean annual frequencies of exceedance. For both the 1 and 10 Hz deaggregations, the licensee determined that local moderate-to-large magnitude earthquakes on the Hosgri fault (i.e., **M**6.0 to **M**8.0 at distances from 0 to 10 km from the DCPP site) dominate the hazard.

STAFF EVALUATION

To evaluate the acceptability of the PSHA, the NRC staff performed a confirmatory evaluation of the seismic sources that contribute most to the hazard at the DCPP. The purpose of the staff's evaluation was to assess the reasonableness of the 1 Hz and 10 Hz mean hazard results for the most significant seismic sources and assess the impact of the most significant source and ground motion parameters on the final hazard results. For this confirmatory analysis, the NRC staff selected a subset of the SSC and GMC branches that focus on the highest weighted components of the logic tree.

The local fault sources selected by the NRC staff for its confirmatory evaluation are the Hosgri, Shoreline, Los Osos, and San Luis Bay faults (see Figure 3.3-1 of this staff assessment). For each of the fault sources, the staff primarily focused on either the Hosgri or the Outward Vergent Fault geometry model and modeled a range of earthquake ruptures on these primary faults using the characteristic earthquake distribution (Youngs and Coppersmith, 1985). Rather than

allocating the fault slip rate amongst the multiple rupture models developed by the TI Team, the staff used a more traditional approach. Specifically, the NRC staff used the 5^{th}, 50^{th}, and 95^{th} percentile slip rates for each individual fault to develop baserock 1 and 10 Hz hazard curves. Figures 3.3-2(a-b) of this staff assessment show the NRC staff's 1 and 10 Hz hazard curves for the Hosgri fault assuming the H90 fault geometry model, a maximum magnitude of 7.4, a fault length of 107 km, a width of 12 km, an equivalent Poisson's ratio of 1.2, and fault slip rates of 0.7, 1.7, and 2.6 mm/yr. For its confirmatory evaluation, the NRC staff used all of the 1 or 10 Hz GMPEs and the central branch for single-station sigma. As shown in Figures 3.3-2(a-b), the staff's confirmatory results assuming the median slip rate closely match the licensee's results for both the 1 Hz and 10 Hz mean hazard curves at the 10^{-4} and 10^{-5} annual frequencies of exceedance, which are used to develop the GMRS.

Figures 3.3-3(a-b) of this staff assessment show the NRC staff's 1 and 10 Hz hazard curves for the Shoreline fault assuming the OV-01 fault geometry model, a maximum magnitude of 6.7, a fault length of 51 km, a width of 12 km, and fault slip rates of 0.03, 0.06, and 0.16 mm/yr. As shown in Figures 3.3-3(a-b), the NRC staff's confirmatory results encompass the licensee's hazard results for both the 1 Hz and 10 Hz mean hazard curves. Similarly, for the Los Osos and San Luis Bay faults, the staff used the OV-07 and OV-05 Outward Vergent rupture models along with the 5^{th}, 50^{th}, and 95^{th} percentile fault slip rates to develop 1 Hz and 10 Hz hazard curves. The staff's confirmatory results for these faults are similar to the licensee's results at the 10^{-4} and 10^{-5} annual frequencies of exceedance even though the SSC TI Team allocated only a portion of the total fault slip rates to these two rupture models. Additionally, the staff notes that these confirmatory calculations, similar to the licensee's calculations, show that the seismic hazard at the DCPP is controlled by the Hosgri fault.

The NRC staff selected the Local source zone for its confirmatory evaluation, which, as the host source zone, contributes moderately to both the 1 and 10 Hz total mean hazard for the DCPP site. For each of the virtual faults modeled in the confirmatory analysis, the NRC staff assumed a maximum magnitude of 6.8, a fault length of 50 km, both reverse and strike-slip faulting, and a spatially uniform recurrence rate. Figure 3.3-4(a-b) of this staff assessment shows the staff's 1 Hz and 10 Hz confirmatory hazard curves for each of the 18 virtual faults, along with the weighted mean hazard curve. As shown in Figure 3.3-4(a-b), the staff's confirmatory results closely match the licensee's mean hazard curves for the Local areal source zone.

In summary, the NRC staff concludes that the licensee acceptably implemented the SSC and GMC logic trees in developing the baserock hazard consistent with the guidance specified in Enclosure 1 to the 50.54(f) letter (NRC, 2012a). Through its confirmatory analyses, the NRC staff was able to confirm the licensee's hazard results. Moreover, the staff's review confirms the reasonableness of the licensee's seismic source and ground motion characterizations. Therefore, the staff concludes that the resulting baserock PSHA hazard curves capture the center, body, and range of the technically defensible interpretations.

3.4 Site Response Evaluation

The DCPP is located on a relatively broad Quaternary terrace surface near the mouth of Diablo Canyon Creek. Bedrock geology of the site consists of the Miocene (5–23 million years ago) Obispo Formation, which is a 400-m thick sequence of thin-to-thickly bedded marine volcanic

and volcaniclastic deposits. The Obispo Formation rests unconformably above highly deformed bedrock, which consists primarily of the Jurassic (144–200 million years ago) Franciscan Formation. The Franciscan Formation is a chaotic mélange of basaltic volcanic rocks (many of which have been altered to greenstone), radiolarian chert, sandstone, limestone, serpentinite, shale, and high-pressure metamorphic rocks.

Attachment 1 to Enclosure 1 of the 50.54(f) letter requests that, after completing PSHA calculations for site baserock conditions, licensees provide a GMRS developed from the site-specific seismic hazard curves at the control point elevation. To develop site-specific hazard curves at the control point elevation, Attachment 1 requests that licensees perform a site response evaluation. In addition, the 50.54(f) letter specifies that the subsurface site response model, for both soil and rock sites, should extend to sufficient depth to reach the baserock conditions as defined for the GMPEs used in the PSHA. For the SWUS GMC models that are used for the DCPP PSHA, baserock conditions are defined for soft rock with a V_{S30} of 760 m/s.

The purpose of the site response analysis is to determine the site amplification that occurs because of baserock ground motions propagating upward through the soil and/or rock column to the surface. The critical parameters that determine what frequencies of ground motion are affected by the upward propagation of baserock motions are the layering of soil and/or soft rock, the thicknesses of these layers, the shear-wave velocities and low-strain damping of the layers, and the degree to which the shear modulus and damping change with higher ground motion amplitudes.

The licensee used two approaches to compute control point hazard curves for the DCPP site. For its initial SHSR submittal to the NRC (PG&E, 2015a), the licensee used an empirical approach that used on-site earthquake recordings to develop a set of site terms, which are ultimately used to adjust the SWUS median GMPEs. Subsequently, in response to RAIs from the NRC staff (PG&E, 2015d), the licensee used the analytical site response approach described in Appendix B of the SPID (EPRI, 2012) to develop site amplification factors. Ultimately, the licensee used a weighted combination of the control point hazard curves from these two approaches (empirical and analytical) to develop the final GMRS for the DCPP. The staff's review of the site data and recordings is provided in Section 3.4.1 of this staff assessment and its confirmatory reviews of the empirical and analytical approaches are described in Sections 3.4.2 and 3.4.3, respectively.

3.4.1 Site Data and Recordings

To develop a set of empirical site term adjustment factors for the median ground motion models, the licensee used on-site recordings in addition to regional recordings of the San Simeon and Parkfield earthquakes. For its analytical site response analysis, the licensee used numerous geophysical datasets and models (Fugro Consultants, 2015) to develop seismic shear wave velocity profiles for the DCPP site.

3.4.1.1 Data for Empirical Approach

The licensee used strong motion recordings from the **M**6.5 2003 San Simeon and the **M**6.0 2004 Parkfield earthquakes to develop the site term adjustment factors for the median ground

motion models. The 2003 San Simeon earthquake occurred on the central coast of California approximately 40 km NNW from the DCPP site, and the 2004 Parkfield earthquake occurred on the San Andreas fault approximately 85 km NNE from the DCPP site (see Figure 3.0-1 of this staff assessment). The San Simeon earthquake was recorded at station ESTA27, which is located to the south of the turbine building where the average shear wave velocity in the upper 30 meters (VS30) is approximately 856 m/s (see Figure 3.4-1 of this staff assessment). After the San Simeon earthquake, an additional station, ESTA28, was installed to the northeast of the turbine building, which has a VS30 of approximately 777 m/s (Figure 3.4-1). Both ESTA27 and ESTA28 recorded the 2004 Parkfield earthquake. In addition to the on-site DCPP recordings, the San Simeon and Parkfield earthquakes were recorded at numerous other strong ground motion recording sites throughout the region. The licensee used a subset of the recordings of the two earthquakes from these other regional sites to estimate the uncertainty in the event-path term for each earthquake, as discussed further in Section 3.4.2 of this staff assessment.

3.4.1.2 Data for Analytical Approach

To perform an analytical site response, the licensee used onsite data from the Power Block 3D Velocity Model (Fugro Consultants, 2015), which was derived from multiple geophysical exploration techniques, including seismic reflection, surface wave dispersion, and downhole suspension logging. The final 3D velocity model combines a high-resolution 3D compressional wave velocity model derived from joint travel time-gravity tomography with an updated 3D shear wave velocity model. This model provided the licensee with a detailed 1 km x 1 km x 600 m volume of shear wave velocity values that it used for the analytical site response.

STAFF EVALUATION OF SITE DATA

The NRC staff notes that in the empirical approach, the licensee was able to directly estimate the site response based on the availability of on-site recordings from two moderately large regional earthquakes. In contrast, more traditional site response methods rely on a simple 1D analysis. However, because this empirical approach has limited data for use in analyzing the DCPP site, the NRC staff requested that the licensee also conduct an analytical site response using available subsurface geophysical data (NRC, 2015e). Specifically, the staff noted that the final empirical site term for the DCPP site is based only on three on-site recordings of two earthquakes. In addition, the staff observed that the source-to-site paths for these two earthquakes are moderately different (NNW for San Simeon and NNE for Parkfield), whereas both of these paths differ significantly from the mainly west-to-east source-to-site paths for the primary faults that contribute the most to the hazard for the DCPP.

To evaluate the tomography model for the DCPP foundation block, the NRC staff developed a 3D velocity model of the DCPP foundation area consisted of compressional and shear-wave velocity structure based on the data compiled in Fugro Consultants (2015). In addition, the NRC staff used a digital elevation model (DEM) and the location of two seismic stations (ESTA27 and ESTA28) that were provided in PG&E (2015d) for the construction of this model. The NRC staff used Petrel software to construct the model, which is a Schlumberger product that is commonly used by the oil and gas industry for subsurface modeling. The DEM used in this analysis consisted of a regular spaced grid that was 2 m by 2 m, and the elevation range was between -57.08 and 426.29 meters above sea level. The NRC staff used a total of

151,003,108 data points to create the velocity model. The range of compressional wave velocity values from the model are 1–2,752 m/s, and the shear wave velocity values ranged from 250–5,791 m/s. The NRC staff's velocity model compares reasonably with the velocity profiles that the licensee relied on to determine the site response. Therefore, the staff concludes that the velocity data relied on by the licensee was adequate for the licensee's site response analysis.

In summary, based on the licensee's utilization of both its on-site recordings of the San Simeon and Parkfield earthquakes as well as abundant site geophysical data, the NRC staff concludes that the combined datasets provide an adequate basis for the licensee's final site response evaluation for the DCPP.

3.4.2 Empirical Site Term Approach

The licensee used the three on-site earthquake recordings of the San Simeon and Parkfield earthquakes to develop a mean site term to estimate the site-specific effects on ground motions due to the local geology underlying the DCPP. The site-specific effects are isolated by first removing the event-specific source and path effects from the GMPEs (which are termed event-corrected GMPEs). Then, the licensee computed the within-event residuals between the event-corrected GMPEs and the on-site recordings. If the within-event residuals computed for separate events are repeatable, then the site term represents the expected deviation in site response from the baserock median GMPEs. To isolate the source and path effects relative to the baserock median GMPEs, the licensee used recordings from eight stations located within 100 km of the San Simeon earthquake epicenter and recordings from sixteen stations located 50 to 150 km from the Parkfield earthquake epicenter. In addition to determining the mean site term, the licensee also estimated the epistemic uncertainty in the site term, which consists of: (1) the uncertainty in the estimated source and path terms for each earthquake; (2) the variability in the single-path within-event residuals; and (3) the variability in the V_{S30} values for stations ESTA27 and ESTA28. The licensee modeled the epistemic uncertainty in the site term by using a three-point weighted distribution for the 5th, median, and 95th percentile values.

STAFF EVALUATION

To evaluate the reasonableness of the DCPP empirical site term, including its empirical uncertainty, the staff performed a confirmatory analysis using the on-site ESTA27 and ESTA28 earthquake records of the San Simeon and Parkfield earthquakes, as well as the recordings of these two earthquakes from other recording stations. As shown in Figure 3.4-2 of this staff assessment, the NRC staff's confirmatory results for the mean site term, as well as the 10 and 90 percent confidence intervals, are reasonably consistent with the licensee's results over the entire frequency range (0.1 Hz to 100 Hz). In addition, based on a comparison of the site term residuals from the San Simeon and Parkfield earthquakes, the NRC staff observes reasonably consistent behavior for the two sets of residuals above the frequency value of 2 Hz. The staff concludes that the consistency of the site term residuals from the two earthquakes demonstrates that the licensee's use of the empirical site term approach successfully identified the site effects for the DCPP. However, as shown in Figure 3.4-2, the site term residuals from the two earthquakes do not follow a consistent trend below 2 Hz. In response to the NRC staff's RAI concerning the inconsistency of the residuals below 2 Hz, the licensee stated that the site

term residuals from the two earthquakes may still contain some source and path effects in addition to the site effects (PG&E, 2015d). Furthermore, the licensee acknowledged that its use of the empirical site term approach is somewhat limited by having only three on-site recordings from two earthquakes and, as such, developed an estimate of the mean site term using an analytical approach.

Based on its review of the licensee's RAI response and the result of the staff's confirmatory analysis, the NRC staff concludes that the empirical approach used by the licensee provides a reasonable estimate of the local site response for frequencies greater than 2 Hz. The staff base this conclusion primarily on the consistency of the site term residuals from the two earthquakes and staff's confirmatory analysis. In addition, the staff concludes that the licensee accurately captured the uncertainty in the site term, which is relatively large due to the small number of available on-site recordings.

3.4.3 Analytical Site Response Evaluation

Because the available dataset used by the licensee for the empirical site term approach is limited, the NRC requested (NRC, 2015c) that the licensee provide site amplification factors in accordance with Appendix B of the SPID guidance. In response to the staff's RAI (PG&E, 2015d), the licensee developed these site amplification factors using an analytical site response approach. The licensee's analytical site response approach provides amplification factors relative to the baserock conditions defined for the SWUS GMC models. The licensee then used these analytical site amplification factors to develop a set of control point hazard curves for the DCPP.

3.4.3.1 Site Basecase Profiles

The licensee used the geometric mean of the 3D shear wave velocity model, described in Section 3.4.1 of this staff assessment, at multiple points beneath the power block and turbine building to develop the upper part of its basecase shear wave velocity profile. The licensee's profile consists of shear wave velocities at 0.5 m intervals from the surface to a depth of 125 m, the range over which its high resolution geophysical data are available. The licensee extended the profile to 900 m based on information provided by Fugro Consultants (2015) and then continued to a depth of 8 km using a reference velocity profiles from the NGA-West2 dataset. To capture the uncertainty in the shear wave velocity beneath the DCPP, the licensee developed lower and upper basecase velocity profiles using a factor of 1.6 times the depth-dependent natural log standard deviation, which the licensee estimated from its 3D model. For the deeper portions of the upper and lower profiles, the licensee used scale factors of 0.9 and 1.1. The licensee assigned weights of 0.6, 0.2, and 0.2, respectively, for the central, upper, and lower profiles. Figure 3.4-3(a) of this staff assessment shows the licensee's three basecase velocity profiles for the upper 125 m and Figure 3.4-3(b) shows the licensee's profiles to 8 km depth. In order to incorporate aleatory variability in the site response analysis, the licensee generated 30 random velocity profiles for each of its basecase profiles such that the resulting profiles capture the range of alternative 3D velocity models.

3.4.3.2 Dynamic Material Properties and Kappa

To model the potential nonlinear behavior in the upper 150 m of strata to input ground motions, the licensee used two sets of shear modulus degradation and damping curves. As recommended in the SPID (EPRI, 2012), the licensee gave equal weight to the EPRI and Peninsular Range curves and limited the amount of damping to 15 percent. In addition, the licensee added a third branch to its site response logic tree to capture the potential for linear behavior. The licensee equally weighted the linear and the two nonlinear responses over the upper 150 m of the profile, such that the linear model has a weight of 0.5 and the EPRI and Peninsular curves each have weights of 0.25. The licensee cited laboratory testing results (PG&E, 1988) of the soft rock at DCPP as a basis for the weights for the three alternative models.

The licensee used the spectral shape from its on-site recording of the Deer Canyon Earthquake (PG&E, 2011) to estimate a kappa value of 0.04 sec for its site response profile. To account for the epistemic uncertainty in kappa, the licensee evaluated the spectral shapes from its on-site recordings of the San Simeon and Parkfield earthquakes in order to constrain the range of kappa values from 0.03 sec to 0.05 sec. Weighting for the three kappa values of 0.03 sec, 0.04 sec, and 0.05 sec is 0.2, 0.6, and 0.2, respectively.

3.4.3.3 Site Amplification Factors

The licensee developed amplification factors for the DCPP profile relative to the surface response spectra for the SWUS baserock condition by using the random vibration theory (RVT) approach recommended by the SPID. To develop input ground motions for the site response analysis, the licensee used a point-source model for a **M**7 earthquake at a depth of 8 km for a range of source-to-site distances. After developing input motions for the site response, the licensee generated 30 random shear wave velocity profiles for each of the three basecase profiles to determine the median site amplification factor and its associated log standard deviation. The licensee limited the site amplification factors to value greater than 0.5 as recommended in the SPID (EPRI, 2012).

STAFF EVALUATION OF ANALYTICAL SITE RESPONSE EVALUATION

Based on its review of the information provided by the licensee in the SHSR (PG&E, 2015a) and the on-site data from the Power Block 3D Velocity Model (Fugro Consultants, 2015), the NRC staff concludes that the licensee's basecase shear wave velocity profiles are consistent with the available subsurface data at the DCPP site. The NRC staff also concludes that the epistemic uncertainty and aleatory variability estimated by the licensee for these profiles are consistent with the geotechnical and geophysical measurements made at the DCPP site. In addition, the NRC staff concludes that the dynamic material property curves used by the licensee are consistent with both the laboratory testing of the near-surface rock (i.e., PG&E, 1988) and the geology of the site, and that the licensee appropriately accounted for uncertainty in the potential nonlinear response by following the guidance provided in the SPID (EPRI, 2012).

To evaluate the licensee's estimate of the kappa value for the site response profile, the NRC staff calculated kappa for each of the on-site DCPP earthquake recordings. Based on these

confirmatory calculations, the NRC staff concludes that the resulting range of kappa values is reasonable. The NRC staff also concludes that the licensee acceptably implemented the point-source model to develop input ground motions, which resulted in a wide range of input motions that appropriately capture the deaggregation results from the PSHA.

The NRC staff performed a confirmatory site response analyses to assess the licensee's site amplification factors. Because of the abundant on-site geophysical datasets developed by the licensee, the NRC staff used the licensee's three basecase velocity profiles. In addition, following the guidance in the SPID, the NRC staff assumed both linear and nonlinear behavior for the materials beneath the DCPP site in response to a range of input motions. Figure 3.4-4 of this staff assessment shows that the NRC staff's confirmatory amplification factors for an input peak ground accelerations of 0.2g and 1.07g closely match the licensee's results.

In summary, based on its evaluation of the SHSR and its confirmatory analysis, the NRC staff concludes that the methods used by the licensee for its site response analysis result in a set of site amplification factors that appropriately characterize the response of the DCPP site to input ground motions.

3.4.4 Control Point Hazard Curves

The licensee used two approaches to compute control point hazard curves for the DCPP site. For its initial SHSR submittal to the NRC (PG&E, 2015a), the licensee used an empirical approach that uses on-site earthquake recordings to develop a set of site terms, which are ultimately used to adjust the SWUS median GMPEs. The licensee then performed a PSHA using these site-adjusted GMPEs to develop control point hazard curves. Subsequently, in response to RAIs from the NRC staff (PG&E, 2015d), the licensee used the analytical site response approach described in Appendix B of the SPID to develop site amplification factors. In order to develop control point hazard curves using the analytical site response amplification factors, the licensee used Approach 3, as described in Appendix B of the SPID (EPRI, 2012). The licensee's use of Approach 3 involved computing the control point elevation hazard curves for a broad range of spectral accelerations by combining the baserock hazard curves, determined from the PSHA (reviewed in Section 3.3 of this staff assessment), and the amplification factors and their associated uncertainties, determined from the site response analysis.

Ultimately, the licensee used a weighted combination of the control point hazard curves from these two approaches (empirical and analytical) to develop the final GMRS for the DCPP. Because the recordings from the on-site stations ESTA27 and ESTA28 for the San Simeon and Parkfield earthquakes provide a direct estimate of the site response for the DCPP, the licensee used a weight of 0.67 for the control point hazard curves developed from the empirical approach. As such, the licensee used a weight of 0.33 for the control point hazard curves developed from the analytical approach.

STAFF EVALUATION

Based on its review of the site response information provided by the licensee in the revised SHSR (PG&E, 2015d) and its confirmatory analyses of the empirical and analytical approaches, the NRC staff concludes that the licensee's final control point hazard curves provide a reasonable characterization of the seismic hazard for the DCPP site. Because the empirical approach relied on a limited amount of on-site recordings from two earthquakes, the NRC staff requested that the licensee perform an analytical site response evaluation that used its abundant on-site geophysical datasets. The NRC staff acknowledges that the analytical approach uses a simplified 1D layered model, which may not fully capture the complexity of the velocity structure beneath the DCPP. Therefore, the NRC staff concludes that the licensee's decision to more heavily weight the empirically derived control point hazard curves is reasonable.

Figure 3.4-5 from the licensee's revised SHSR (PG&E, 2015d) shows the 10^{-4} and 10^{-5} annual exceedance frequency uniform hazard response spectra (UHS) from the empirical and analytical approaches. The main difference between the two UHS is the site resonance near 2 Hz that is captured by the empirical approach, but not by the analytical approach. The NRC staff notes that the licensee's decision to more heavily weight the empirical approach retains this 2 Hz amplification as part of the final GMRS for the DCPP.

In summary, based on its evaluation of the SHSR, PG&E's RAI responses, and its confirmatory analysis, the NRC staff concludes that the methods used by the licensee for its site response analysis result in a set of control point hazard curves that appropriately characterize the seismic hazard of the DCPP site and are appropriate for use in the PSHA.

3.5 GMRS and Screening Results

3.5.1 Plant Seismic Design Basis

Enclosure 1 of the 50.54(f) letter (NRC, 2012a) requested that the licensee provide the SSE ground motion values, as well as the specification of the control point elevation(s), for comparison to the GMRS. For operating power reactors with construction permits issued before 1997, the SSE is the plant licensing basis earthquake and is characterized by: (1) a peak ground acceleration (PGA) value that anchors the response spectra at high frequencies (typically at 20 Hz to 30 Hz for the existing fleet of nuclear power plants); (2) a response spectrum shape that depicts the amplified response at all frequencies below the PGA; and (3) a control point location where the SSE is defined.

In Section 3.1 of its SHSR (PG&E, 2015a), the licensee described its seismic design bases for DCPP site. For the purposes of the 50.54(f) response, the licensee stated that the SSE for DCPP is the DDE, which is anchored at a PGA of 0.4g (PG&E, 2013a). Because the Updated Final Safety Analysis Report (UFSAR) does not explicitly define an SSE control point (PG&E, 2013b), the licensee used information from seismic analysis in the UFSAR to determine that the control point is at finished grade level for the major structures at DCPP. This control point corresponds to an elevation of 26 m mean sea level, which the licensee used in its site response evaluations.

The NRC staff reviewed the licensee's description of the SSE in the SHSR for the DCPP site. Based on review of the licensing basis contained in the UFSAR for DCPP (PG&E, 2013b), the NRC staff confirms that the licensee's SSE is a 5 percent damped response spectrum anchored at 0.4g, which is represented by the DDE. Finally, based on review of the SHSR and the UFSAR, the NRC staff confirms that the licensee's control point elevation for the DCPP SSE is consistent with the guidance provided in the SPID (EPRI, 2012).

3.5.2 Screening Comparison

The GMRS is used to represent the free-field seismic hazard at the control point elevation. To calculate the GMRS, the licensee first used site-specific rock hazard curves from the PSHA (reviewed in Section 3.3 of this staff assessment) and the site term adjustment factors (reviewed in Section 3.4) to calculate control point hazard curves. The licensee then used these curves to develop 10^{-4} and 10^{-5} (mean annual frequency of exceedance) uniform hazard response spectra, and then computed the GMRS using the criteria in Regulatory Guide 1.208 (NRC, 2007). In response to RAIs, the licensee updated the GMRS initially submitted in PG&E (2015a) to incorporate additional information in the DCPP site response (PG&E, 2015d). The licensee's initial and updated horizontal GMRS for the DCPP site are shown in Figure 3.5-1 of this staff assessment.

To review the licensee's GMRS, the staff relied on the results of the reviews documented in Sections 3.1 to 3.4 of this staff assessment. Based on the result of its review, the staff determined that the licensee developed acceptable site-specific rock hazard curves that represented a reasonable implementation of the SSC and GMC models in the PSHA. The staff also determined in Section 3.4 that the licensee developed acceptable site term adjustment factors, which it then used to calculate control-point hazard curves. In particular, the staff determined that the licensee used an acceptable approach to update the initially submitted GMRS in response to additional information. The staff also determined that the licensee used appropriate criteria in RG 1.208 to calculate the GMRS.

Based on the assessment of the licensee's SHSR and the responses to RAIs, the staff confirms that the licensee used present-day guidance and methodologies outlined in Regulatory Guide 1.208 and the SPID to calculate the horizontal GMRS, as requested in the 50.54(f) letter. Based on the results of its review, the NRC staff concludes that the GMRS determined by the licensee adequately characterizes the reevaluated seismic hazard for the DCPP site. Therefore, this GMRS is suitable for use in subsequent evaluations and confirmations, as needed, for the response to the 50.54(f) letter (NRC, 2012a).

4.0 CONCLUSION

The NRC staff reviewed the information provided by the licensee for the reevaluated seismic hazard for the DCPP site. Based on this review, the NRC staff concludes that the licensee conducted the seismic hazard reevaluation using present-day methodologies and regulatory guidance, it appropriately characterized the DCPP site given the information available, and met the intent of the guidance for determining the reevaluated seismic hazard. Based upon the preceding analysis, the NRC staff concludes that the licensee's SHSR provided an acceptable

response to Requested Information Items (1) – (3) and (5) – (7), and the comparison portion to Item (4), identified in Enclosure 1 of the 50.54(f) letter.

In reaching this conclusion, the NRC staff confirmed the licensee's conclusion that the licensee's GMRS exceeds the SSE at the DCPP site. As such, the licensee will perform a seismic risk evaluation, SFP evaluation, and high frequency confirmation, consistent with the schedule in the NRC screening and hazard results for the WUS sites (NRC, 2015a). The NRC staff's review and acceptance of PG&E's plant seismic risk evaluation, including the high frequency confirmation, and SFP evaluation (i.e., Items (4), (8), and (9)) for the DCPP site will complete the seismic hazard reevaluation identified in Enclosure 1 of the 50.54(f) letter (NRC, 2012a).

5.0 REFERENCES

Note: ADAMS Accession Nos. refers to documents available through NRC's Agencywide Documents Access and Management System (ADAMS). Publicly-available ADAMS documents may be accessed through http://www.nrc.gov/reading-rm/adams.html.

U.S. Nuclear Regulatory Commission Documents and Publications

NRC (U.S. Nuclear Regulatory Commission), 1991, "Safety Evaluation Report related to the operation of Diablo Canyon Nuclear Power Plant, Units 1 and 2 Docket Nos. 50-275 and 50-323," NUREG-0675, Sup. 34, ADAMS Accession No. ML093070113.

NRC, 2007, A Performance-based Approach to Define the Site-Specific Earthquake Ground Motion, Regulatory Guide (RG) 1.208, March 2007, ADAMS Accession No. ML070310619.

NRC, 2011a, "Recommendations for Enhancing Reactor Safety in the 21st Century: The Near-Term Task Force Review of Insights from the Fukushima Dai-Ichi Accident," Enclosure to SECY-11-0093, July 12, 2011, ADAMS Accession No. ML11186A950.

NRC, 2011b, "Near-Term Report and Recommendations for Agency Actions Following the Events in Japan," Commission Paper SECY-11-0093, July 12, 2011, ADAMS Accession No. ML11186A950.

NRC, 2011c, "Recommended Actions to be Taken Without Delay from the Near-Term Task Force Report," Commission Paper SECY-11-0124, September 9, 2011, ADAMS Accession No. ML11245A158.

NRC, 2011d, "Prioritization of Recommended Actions to be Taken in Response to Fukushima Lessons Learned," Commission Paper SECY-11-0137, October 3, 2011, ADAMS Accession No. ML11272A111.

NRC, 2012a, letter from Eric J. Leeds, Director, Office of Nuclear Reactor Regulation and Michael R. Johnson, Director, Office of New Reactors, to All Power Reactor Licensees and Holders of Construction Permits in Active or Deferred Status, March 12, 2012, ADAMS Accession No. ML12053A340.

NRC, 2012b, "Central and Eastern United States Seismic Source Characterization for Nuclear Facilities," NUREG-2115, ADAMS stores the NUREG as multiple ADAMS documents, which are accessed through the webpage http://www.nrc.gov/reading-rm/doc-collections/nuregs/staff/sr2115/.

NRC, 2012c, "Research Information Letter 12-01, Confirmatory Analysis of Seismic Hazard at the Diablo Canyon Power Plant from the Shoreline Fault Zone," ADAMS Accession No. ML121230035.

NRC, 2012c, "Practical Implementation Guidelines for SSHAC Level 3 and 4 Hazard Studies," NUREG-2117, ADAMS Accession No. ML12118A445.

NRC, 2013a, Letter From Eric J. Leeds, to Joseph Pollock, Executive Director NEI, Acceptance Letter for NEI Submittal of Augmented Approach, Ground Motion Model Update Project, and 10 CFR 50.54(f) Schedule Modifications Related to the NTTF Recommendation 2.1, Seismic Reevaluations, May 7, 2013, ADAMS Accession No. ML13106A331.

NRC, 2013b, letter from Eric J. Leeds, Director, Office of Nuclear Reactor Regulation, to Joseph E. Pollock, Executive Director, Nuclear Energy Institute, Endorsement of Electric Power Research Institute Draft Report 1025287, "Seismic Evaluation Guidance," February 15, 2013, ADAMS Accession No. ML12319A074.

NRC, 2015a, Letter from W. M. Dean (NRC) to Licensees of the Columbia Generating Station, Diablo Canyon Power Plant and Palo Verde Nuclear Generating Station, Screening and Prioritization Results for the Western United States sites Regarding Information Pursuant to Title 10 of the Code of Federal Regulations 50.54(f) Regarding Seismic Hazard Reevaluations for Recommendations 2.1 of the Near-Term Task Force Review of Insights from the Fukushima Dai-ichi Accident, May 13, 2015, ADAMS Accession No. ML15113B344.

NRC, 2015b, Letter from W.M. Dean (NRC) to Licensees, Final Determination of Licensee Seismic Probabilistic Risk Assessments Under the Request for Information Pursuant to Title 10 of the Code of Federal Regulations 50.54(F) Regarding Recommendation 2.1 "Seismic" of the Near-Term Task Force Review of Insights from the Fukushima Dai-Ichi Accident, October, 27, 2015, ADAMS Accession No. ML15194A015.

NRC, 2015c, Letter from N. J. DiFrancesco (NRC) to E. D. Halpin, Diablo Canyon Power Plant, Unit Nos. 1 and 2 - Request for Additional Information Associated with Near-Term Task Force Recommendation 2.1, Seismic Reevaluations (TAC Nos. MF5275 AND MF5276), June 29, 2015, ADAMS Accession No. ML15153A033.

NRC, 2015d, Letter from F.G. Vega (NRC) to E. D. Halpin, Diablo Canyon Power Plant, Unit Nos. 1 and 2 - Request for Additional Information Associated with Near-Term Task Force Recommendation 2.1, Seismic Reevaluations, August 27, 2015, ADAMS Accession No. ML15238B774.

NRC, 2015e, Letter from N. J. Difrancesco (NRC) to E. D. Halpin, Diablo Canyon Power Plant, Unit Nos. 1 and 2 - Request for Additional Information Associated with Near-Term Task Force Recommendation 2.1, Seismic Reevaluations, October 1, 2015, ADAMS Accession No. ML15267A774.

NRC, 2015f, Email from N. DiFrancesco (NRC) to P. Soenen (DCPP), Subject: Information Request Related to Diablo Canyon Regulatory Audit of the Reevaluated Seismic Hazard, November 13, 2015, ADAMS Accession No. ML15323A200.

Other References

Abrahamson, N. A., W. J. Silva, and R. Kamai, 2014, "Update of the AS08 Ground-Motion Prediction Equations Based on the NGA-West2 Data Set," *Earthquake Spectra* 30(3): 1,025–1,055.

Akkar, S., M. A. Sandikkaya, and J. J. Bommer, 2014, "Empirical ground-motion models for point- and extended-source crustal earthquake scenarios in Europe and the Middle East," *Bulletin of Earthquake Engineering*, 12(1): 359–387.

Ancheta, T.D., and 11 others, 2014, "NGA-West 2 Database," *Earthquake Spectra*, 30(3): 989–1,005.

Argus, D. F. and R. G. Gordon, 2001, "Present tectonic motion across the Coast Ranges and San Andreas fault system in central California," *Geological Society of America Bulletin,* 113 (12): 1,580–1,592.

Atwater, T., 1989, "Plate Tectonic History of the Northeast Pacific and Western North America" (E. L. Winterer, D. M. Hussong, and R. W. Decker, eds.), *The Eastern Pacific Ocean and Hawaii, The Geology of North America,* Vol. N: 21–71.

Biasi, G. P., R. J. Weldon II, T. E. Fumal, and G. G. Seitz, 2002, "Paleoseismic event dating and the conditional probability of large earthquakes on the southern San Andreas fault, California," *Bulletin of the Seismological Society of America*, 92 (7): 2,761–2,781.

Bird, P., 2012, "NeoKinema Fault-Based Deformation Model of the California Region for UCERF3, with Focus on the DCPP Region," presentation at DCPP SSHAC Workshop #2, November 7; available at http://www.pge.com/mybusiness/edusafety/systemworks/dcpp/SSHAC/workshops/index.shtml.

Boore, D. M., J. P. Stewart, E. Seyhan, and G. M. Atkinson, 2014, "NGA-West2 Equations for Predicting Response Spectral Accelerations for Shallow Crustal Earthquakes," *Earthquake Spectra,* 30(3): 1,057–1,085.

Bozorgnia, Y., and 32 others, 2014, "NGA-West2 research project," *Earthquake Spectra,* 30: 973–987.

Budnitz, R.J., G. Apostolakis, D. M. Boore, L. S. Cluff, K. J. Coppersmith, C. A. Cornell and P. A. Morris, 1997, "Recommendations for probabilistic seismic hazard analysis: guidance on uncertainty and the use of experts," NUREG/CR-6372, two volumes, US Nuclear Regulatory Commission, Washington, D.C., ADAMS Accession No. ML080090003.

CSUMB (California State University, Monterey Bay, Sea Floor Mapping Lab), 2012, "Multibeam echo sounder (MBES) data for the California Central Coast," available at http://seafloor.csumb.edu/SFMLwebDATA_c.htm

Campbell, K. W., and Y. Bozorgnia, 2014, "NGA-West2 Campbell-Bozorgnia Ground Motion Model for the Horizontal Components of PGA, PGV, and 5%-Damped Elastic Pseudo-Acceleration Response Spectra for Periods Ranging from 0.01 to 10 sec," *Earthquake Spectra* 30(3): 1,087–1,115.

Chiou, B. S.-J., and R. R. Youngs, 2014, "Update of the Chiou and Youngs NGA Ground Motion Model for Average Horizontal Component of Peak Ground Motion and Response Spectra," *Earthquake Spectra* 30(3): 1,117–1,153.

Clark, D. H., N. T. Hall, D. H. Hamilton, and R. G. Heck, 1991, "Structural analysis of late Neogene deformation in the central offshore Santa Maria Basin, California," *Journal of Geophysical Research* 96 (B4): 6,435–6,457.

DeMets, C., 2012, "Final report: Kinematics of coastal California inferred from GPS geodesy," unpublished technical report submitted to Pacific Gas and Electric Company, December: 21 pp.

DeMets, C., B. Márquez-Azúa, E. Cabral-Cano, 2014, "A new GPS velocity field for the Pacific Plate – Part 2: implications for fault slip rates in western California," *Geophysical Journal International* 199 (3): 1,900–1,909.

EPRI (Electric Power Research Institute), 1988, EPRI Report NP-4726-A, "Seismic Hazard Methodology for the Central and Eastern United States," Volumes 1-10, Palo Alto, California.

EPRI, 2012, EPRI Report 1025287 "Seismic Evaluation Guidance, Screening, Prioritization and Implementation Details [SPID] for the Resolution of Fukushima Near-Term Task Force Recommendation 2.1: Seismic," November 27, 2012, ADAMS Accession No. ML12333A170.

Field, E. H., and 10 others, 2009, "Uniform California Earthquake Rupture Forecast, Version 2 (UCERF2)," *Bulletin of the Seismological Society of America*, 99(4): 2,053–2,107.

Field, E. H., and 17 others, 2013, "Uniform California Earthquake Rupture Forecast, Version 3 (UCERF3)—The Time-Independent Model," *U.S. Geological Survey Open-File Report 2013–165.*

Fitzenz, D. D., M. A. Ferry, and A. Jalobeanu, 2010, "Long-term slip history discriminates among occurrence models for seismic hazard assessment," *Geophysical Research Letters*, 37(2): L20307.

Fugro Consultants, 2015, "Update of the Three-Dimensional Velocity Model for the Diablo Canyon Power Plant (DCPP) Foundation Area," technical report to PG&E, May 2015.

GeoPentech, 2015, "Southwestern United States Ground Motion Characterization SSHAC Level 3 – Technical Report, Rev.2," March 2015.

Gutenberg, B., and Richter, C. F., 1944, "Frequency of earthquakes in California," *Bulletin of the Seismological Society of America*, 34: 185–188.

Hall, C. A., Jr., 1973, "Geologic Map of the Morrow Bay South and Port San Luis Quadrangles, San Luis Obispo County, California," *U.S. Geological Survey Miscellaneous Field Studies Map* MF-511, Scale 1:24,000.

Hanks, T. C., and W. H. Bakun, 2008, "M—log A observations for recent large earthquakes," *Bulletin of the Seismological Society of America*, 98: 490–494.

Hanks, T. C., and Bakun, W. H., 2014, "M–log A models and other curiosities," *Bulletin of the Seismological Society of America*, 104(5): 2,604–2,610.

Hanson, K. L., W. R. Lettis, M. K. McLaren, W. U. Savage, and N. T. Hall, 2004, "Style and rate of Quaternary deformation of the Hosgri fault zone, offshore south-central California," (M. A. Keller, ed.), *Evolution of Sedimentary Basins/Onshore Oil and Gas Investigations—Santa Maria Province, U.S. Geological Survey Bulletin 1995-BB*, 33 pp.

Hanson, K. L., J. R. Wesling, W. R. Lettis, K. I. Kelson,, and L. Mezger, 1994, "Correlation, Ages, and Uplift Rates of Quaternary Marine Terraces, South-Central California," (I. B. Alterman, R. B. McMullen, L. S. Cluff, and D. B. Slemmons, eds) *Seismotectonics of the Central California Coast Range, Geological Society of America Special Paper* 292: 45–72.

Hardebeck, J. L., 2010, "Seismotectonics and fault structure of the California central coast," *Bulletin of the Seismological Society of America* 100(3): 1,031–1,050.

Hardebeck, J. L., 2013, "Geometry and earthquake potential of the Shoreline Fault, Central California," *Bulletin of the Seismological Society of America* 103(1): 447–462.

Hardebeck, J. L., 2014, "Seismicity and Fault Structure of Estero Bay and the Irish Hills," presentation at DCPP SSHAC Workshop 3, March 26, available at http://www.pge.com/mybusiness/edusafety/systemworks/dcpp/SSHAC/workshops/index.shtml.

Hartwell, S. R., D. P. Finlayson, P. Dartnell, and S. Y. Johnson, 2013, "Bathymetry and acoustic backscatter—Estero Bay, California, U.S.," *Geological Survey Open-File Report 2013–1225*.

Idriss, I.M., 2014, "An NGA-West2 empirical model for estimating the horizontal spectral values generated by shallow crustal earthquakes," *Earthquake Spectra*, 30(3): 1,155–1,177.

Johnson, S.Y., and J. T. Watt, 2012, "Influence of fault trend, bends, and convergence on shallow structure and geomorphology of the Hosgri strike-slip fault, offshore central California," *Geosphere* 8(6): 1,632–1,656.

Johnson, S. Y., S. R. Hartwell, and P. Dartnell, 2014, "Offset of latest Pleistocene shoreface reveal slip rate on the Hosgri strike-slip fault, offshore central California," *Bulletin of the Seismological Society of America* 104 4): 1,650–1,662.

Keithline, 2012, Letter from Kimberly Keithline, Senior Project Manager, NEI, to David L. Skeen, Director, Japan Lessons Learned Project Directorate, NRC, "Final Draft of Industry Seismic Evaluation Guidance (EPRI 1025287)," November 27, 2012, ADAMS Accession No. ML12333A168.

Langenheim, V. E., R. C. Jachens, and K. Moussaoui, 2009, "Aeromagnetic Survey Map of the Central California Coast Ranges," *U.S. Geological Survey Open-File Report 2009-1044*.

Lettis, W.R., and N. T. Hall, 1994, "Los Osos fault zone, San Luis Obispo County, California," (I. B. Alterman, R. B. McMullen, L. S. Cluff, and D. B. Slemmons, ed), *Seismotectonics of the Central California Coast Ranges, Geological Society of America Special Paper 292*, pp. 73–102.
Lettis, W. R. and K. L. Hanson, 1991, "Crustal strain partitioning; implications for seismic hazard assessment in western California," *Geology*, 19: 559–562.

Lettis, W. R., K. L. Hanson, J. R. Unruh, M. McLaren, and W. U. Savage, 2004, "Quaternary Tectonic setting of south-central coastal California," (M. A. Keller, ed.) *Evolution of Sedimentary Basins/Offshore Oil and Gas Investigations—Santa Maria Province, U.S. Geological Survey Bulletin 1995-AA:* 1–21.

Lin, J., and R. S. Stein, 2004, "Stress triggering in thrust and subduction earthquakes and stress interaction between the southern San Andreas and nearby thrust and strike-slip faults," *Journal of Geophysical Research*, 109(B2): 2,156–2,202.

Lin, P. -S., B. Chiou, N. Abrahamson, M. Walling, C. -T. Lee, and C. -T. Cheng, 2011, "Repeatable source, site, and path effects on the standard deviation for empirical ground-motion prediction models," *Bulletin of the Seismological Society of America*, 101(5): 2,281–2,295.

Maechling, P. J., F. Silva, S. Callaghan, and T. H. Jorda, 2015, "Broadband platform: System architecture and software implementation," *Seismological Research Letters*, 86(1): 27–38.

McGinnis, R. N., A. P. Morris, D. A. Ferrill, K. J. Smart, J. A. Stamatakos, and M. R. Juckett, 2016, "Independent evaluation of the Hosgri Fault slip rate based on a structural analysis of the pull-apart basin linking the Hosgri and San Simeon Fault systems," Center for Nuclear Waste Regulatory Analyses: TX, 40p. ADAMS Accession No. ML16334A406.

McLaren, M. K. and Savage, W. U., 2001, "Seismicity of south-central coastal California: October 1987 through January 1997," *Bulletin of the Seismological Society of America,* 91(6): 1,629–1,658.

McLaren, M. K ., J. L. Hardebeck, N. van der Elst, J. R. Unruh, G. W. Bawden, and J. L. Blair, 2008, "Complex faulting associated with the 22 December 2003 Mw 6.5 San Simeon, California Earthquake, aftershocks and postseismic surface deformation," *Bulletin of the Seismological Society of America* 98(4): 1,659–1,680.

Muhs, D. R., K. R. Simmons, R. R. Schumann, L. T. Groves, D. Laurel, and J. X. Mitrovica, 2012, "Sea-level history during the Last Interglacial complex on San Nicolas Island, California: Implications for glacial isostatic adjustment processes, paleozoogeography and tectonics," *Quaternary Science Reviews* 37: 1–25.

Murray, R. W., 2012, "Regional Deformation and Kinematics from GPS Data," presentation at DCPP SSHAC Workshop 2, November 7; available at http://www.pge.com/mybusiness/edusafety/systemworks/dcpp/SSHAC/workshops/index.shtml.

Petersen, M. D., C. S. Mueller, A. D. Frankel, and Y. Zeng, 2008, "Appendix J—Spatial Seismicity Rates and Maximum Magnitudes for Background Earthquakes," (E. H. Field and 10 others, eds.), *The Uniform California Earthquake Rupture Forecast, Version 2 (UCERF 2), USGS Open File Report 2007-1437.*

Pietrangelo, 2013, Letter from A. R. Pietrangelo (NEI) to D. L. Skeen (NRC), "Proposed Path Forward for NTTF Recommendation 2.1: Seismic Reevaluations," April 9, 2013, ADAMS Accession No. ML13101A379.

PG&E (Pacific Gas & Electric Company), 1988, "Final Report of the Diablo Canyon Long-Term Seismic Program, Report to the U.S. NRC," Docket Nos. 50-275 and 50-323.

PG&E, 1991a, "PG&E Letter No. DCL-91-027, Addendum to the 1988 Final Report of the Diablo Canyon Long Term Seismic Program," February 13, 1991, Docket Nos. 50-275 and 50-323.

PG&E, 1991b, "PG&E Letter No. DCL-91-091, Benefits and Insights of the Long-Term Seismic Program," April 17, 1991, Docket Nos. 50-275 and 50-323.

PG&E, 1991c, "PG&E Letter No. DCL-91-143, Long-Term Seismic Program— Implementation of the Results of the Program," May 29, 1991, Docket Nos. 50-275 and 50-323.

PG&E, 2011, "Report on the Analysis of the Shoreline Fault Zone, Central Coastal California, Report to the U.S. Nuclear Regulatory Commission," ADAMS Accession No. ML110140431.

PG&E, 2013a, Letter from Barry Allen, Site Vice President, to U. S. Nuclear Regulatory Commission, Diablo Canyon Units 1 and 2 Docket Nos. 50-275 and 50-323, Response to NRC Request for Information Pursuant to 10 CFR 50.54(f) Regarding the Seismic Aspects of Recommendations 2.1 of the Near-Term Task Force Review of Insights from the Fukushima Dai-ichi Accident, April 29, 2013, ADAMS Accession No. ML13120A275.

PG&E, 2013b, "Diablo Canyon Power Plant Units 1 and 2, Final Safety Analysis Report Update, Revision 21," September 2013, ADAMS Accession No. ML15098A453.

PG&E, 2013c, "Stratigraphic Framework for Assessment of Fault Activity Offshore of the Central California Coast between Point San Simeon and Point Sal," PG&E Technical Report GEO.DCPP.TR.13.01, 76 pp.

PG&E, 2014, "Central Coastal California Seismic Imaging Project (CCCSIP)," report to the California Public Utilities Commission; available at http://www.pge.com/en/safety/systemworks/dcpp/seismicsafety/report.page.

PG&E, 2015a, Letter from Barry Allen, Vice President, Nuclear Services, to the NRC, Diablo Canyon Units 1 and 2 Docket Nos. 50-275 and 50-323, Response to NRC Request for Information Pursuant to 10 CFR 50.54(f) Regarding the Seismic Aspects of Recommendation 2.1 of the Near-Term Task Force Review of Insights from the Fukushima Dai-ichi Accident: Seismic Hazard and Screening Report, March 11, 2015, ADAMS Accession No. ML15071A046.

PG&E, 2015b, Letter from Barry Allen, Vice President, Nuclear Services, to the NRC, Diablo Canyon, Units 1 and 2, "Response to NRC Request for Additional Information Regarding Recommendation 2.1 of the Near-Term Task Force Seismic Hazard and Screening Report," August 12, 2015, ADAMS Accession No. ML15224B575.

PG&E, 2015c, Letter from Barry Allen, Vice President, Nuclear Services, to the NRC, "Diablo Canyon, Units 1 and 2- Response to NRC Request for Additional Information dated August 27, 2015, Regarding Recommendation 2.1 of the Near-Term Task Force Seismic Hazard and Screening Report," September 16, 2015, ADAMS Accession No. ML15259A600.

PG&E, 2015d, Letter from L. Jearl Strickland, Director, Technical Services, to the NRC, "Diablo Canyon Units 1 and 2, Response to NRC Request for Additional Information dated October 1, 2015 and November 13, 2015, Regarding Recommendation 2.1 of the Near-Term Task Force Seismic Hazard and Screening Report, December 21, 2015, ADAMS Accession Nos. ML15355A550 and ML15355A551.

PG&E, 2015e, "Seismic Source Characterization for the Diablo Canyon Power Plant, San Luis Obispo County, California; report on the results of a SSHAC Level 3 study," Rev. A, March. Available online at http://www.pge.com/dcpp-ltsp.

PNNL (Pacific Northwest National Laboratory), 2014, "Hanford Sitewide Probabilistic Seismic Hazard Analysis," Report # PNNL-23361, Pacific Northwest National Laboratory, Richland, Washington.

Sammon, J. W., 1969, "A nonlinear mapping for data structure analysis," *IEEE Transactions on Computers,* C-18: 401–409.

Scharer, K.M., G. P Biasi, R. J.Weldon II, and T. E. Fumal, 2010, "Quasi-periodic recurrence of large earthquakes on the southern San Andreas fault," *Geology,* 38 (6): 555–558.

Sieh, K. E., and R. H. Jahns, 1984, "Holocene activity of the San Andreas fault at Wallace Creek. California," *Geological Society of America Bulletin*, 95(8): 883-896.

Sliter, R. W., P. J. Triezenberg, P. E. Hart, J. T. Watt S. Y. Johnson, and D. S. Scheirer, 2010, "High-Resolution Seismic Reflection and Marine Magnetic Data Along the Hosgri Fault Zone, Central California, U.S." *U.S. Geological Survey Open-File Report 2009-1100*, version 1.1.

Steritz, J. W., and B. P. Luyendyk, 1994, "Hosgri Fault Zone, Offshore Santa Maria Basin, California," *Geological Society of America Special Paper 292*, p. 191–209.

Titus, S. J., C. DeMets., and B. Tikoff, 2005, "New slip rate estimates for the creeping segment of the San Andreas Fault, California," *Geology,* 33(3): 205–208.

Titus, S. J., M. Dyson, C. DeMets, B. Tikoff, F. Rolandone, and R. Bürgmann, 2011, "Geologic versus geodetic deformation adjacent to the San Andreas Fault, Central California," *Geological Society of America Bulletin*, 123(5-6): 794–820.

Toda, S., R .S. Stein, K. Richards-Dinger, and S. B. Bozkurt, 2005, "Forecasting the evolution of seismicity in southern California: Animations built on earthquake stress transfer," *Journal of Geophysical Research*, 110(B5): 2,156–2,202.

Toké, N .A., J. R. Arrowsmith, M. J. Rymer, A. Landgraf, D. E. Haddad, M. Busch, J. Coyan, and A. Hannah, 2011, "Late Holocene slip rate of the San Andreas fault and its accommodation by creep and moderate-magnitude earthquakes at Parkfield, California," *Geology*, 39(3): 243–246.

U.S. *Code of Federal Regulations*, "Domestic Licensing of Production and Utilization Facilities," Part 50, Chapter I, Title 10, "Energy."

U.S. *Code of Federal Regulations*, "Reactor Site Criteria," Part 100, Chapter I, Title 10, "Energy."

USGS (U.S. Geological Survey), 2006, Quaternary fault and fold database for the United States, accessed August 22, 2013, from USGS web site: http//earthquakes.usgs.gov/regional/qfaults/.

Youngs, R. R., and K. J. Coppersmith, 1985, "Implications of fault slip rates and earthquake recurrence models to probabilistic seismic hazard estimates," *Bulletin of the Seismological Society of America,* 75(4): 939–964.

Waldhauser, F. and W. L. Ellsworth, 2000, "A double-difference earthquake location algorithm: Method and application to the northern Hayward fault, California," *Bulletin of the Seismological Society of America*, 90(6): 1,353–1,368.

Wesnousky, S. G., C. H. Scholz, K. Shimazaki, and T. Matsuda, 1983, "Earthquake frequency distribution and the mechanics of faulting," *Journal of Geophysical Research*, 88: 9,331–9,340.

Willingham, C. R., J. D. Rietman, R. G. Heck, and W. R. Lettis, 2013, "Characterization of the Hosgri Fault Zone and Adjacent Structures in the Offshore Santa Maria Basin, South Central California," (M. A. Keller, ed.), *Evolution of Sedimentary Basins/Onshore Oil and Gas Investigations—Santa Maria Province, U.S. Geological Survey Bulletin 1995-CC,* 105p.

Wooddell, K., 2011, "Sensitivity Studies," presentation at DCPP SSHAC Workshop 1, November 29; available at http://www.pge.com/mybusiness/edusafety/systemworks/dcpp/SSHAC/workshops/index.shtml.

Youngs, R. R., and K. J. Coppersmith, 1985, "Implications of fault slip rates and earthquake recurrence models to probabilistic seismic hazard estimates," *Bulletin of the Seismological Society of America,* 75(4): 939–964.

Zhang, H., and C. H. Thurber, 2003, "Double-difference tomography: The method and its application to the Hayward Fault, California," *Bulletin of the Seismological Society of America,* 93(5): 1,875–1,889.

Zhao, J. X., and 8 others, 2006, "Attenuation relations of strong ground motion in Japan using site classification based on predominate period," *Bulletin of the Seismological Society of America*, 96: 898–913.

Zhao, J. X., and M. Lu, 2011, "Magnitude-Scaling Rate in Ground-Motion Prediction Equations for Response Spectra from Large, Shallow Crustal Earthquakes," *Bulletin of the Seismological Society of America*, 101: 2,643–2661.

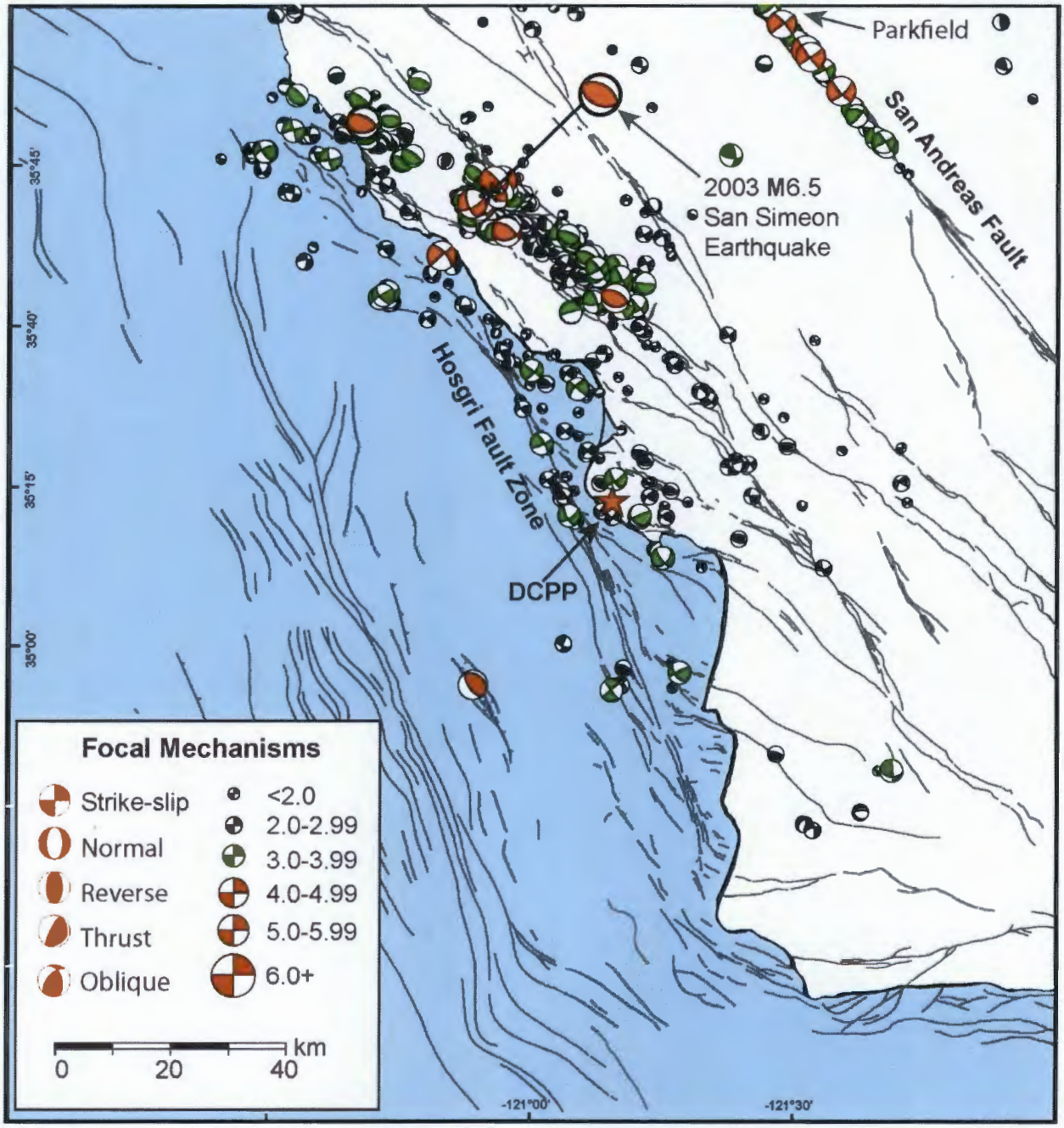

Figure 3.0-1. Seismicity patterns and focal mechanisms of the DCPP region based on Hardebeck (2010) for events between 1987 and 2008. Redrafted from Figure 5-24 of PG&E (2015e).

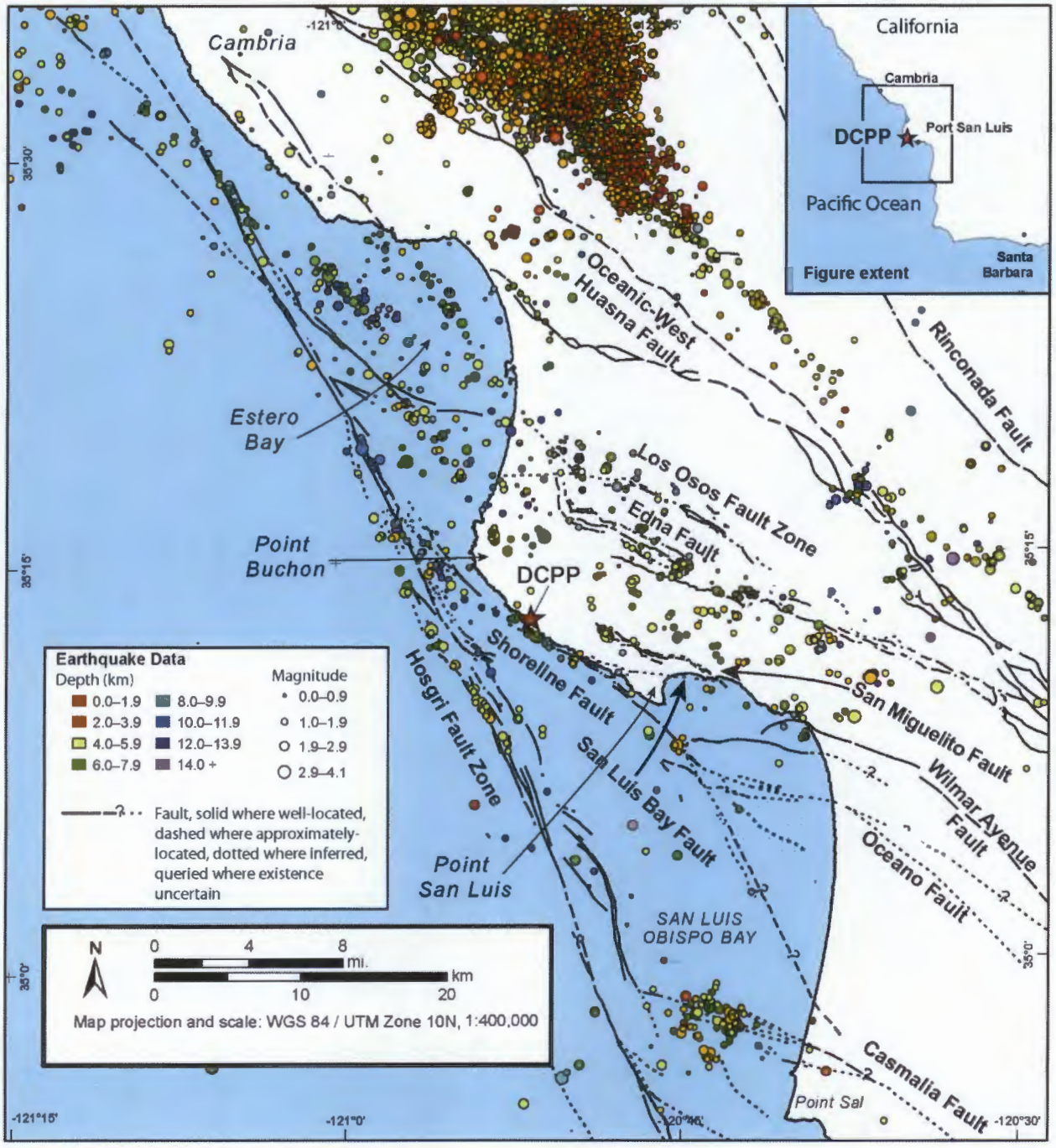

Figure 3.0-2. Regional seismicity patterns from 1987 to 2013 relative to the mapped traces of known faults, redrafted from Figure 5-16 of PG&E (2015e).

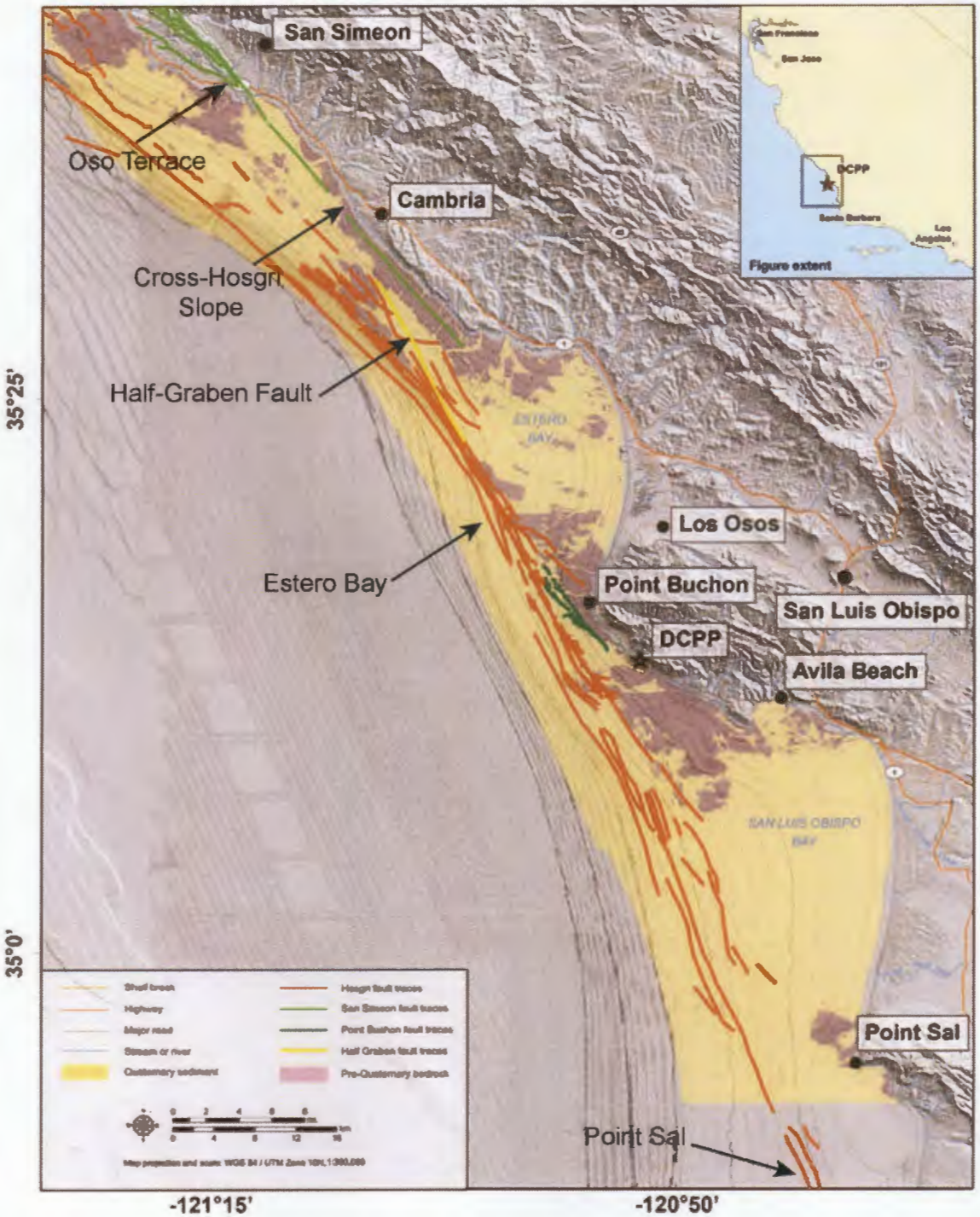

Figure 3.1-1. Locations where slip rates for the Hosgri fault were determined, including the trace of the Half Graben Fault. Modified From Figure 1.2-1 of PG&E (2014), in McGinnis et al. (2016).

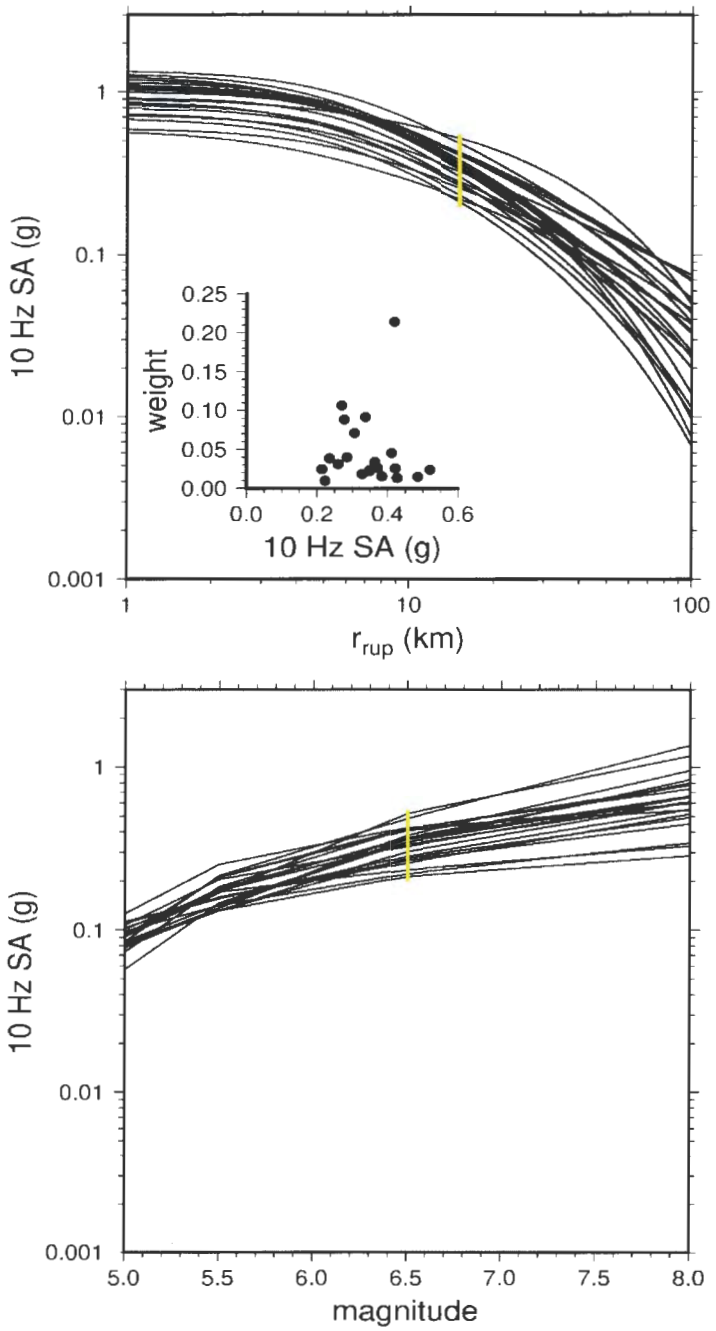

Figure 3.2-1. (a) Distribution of weighted medians produced from the 22 GMPEs using the Sammon's map approach for the local sources, for a spectral period of 0.1 seconds for a **M**6.5 earthquake for source-to-site distances ranging from 1 to 100 km. Inset shows the weighted distribution of median spectral accelerations for a **M**6.5 earthquake at a source-to-site distance of 15 km. (b) The same GMPEs for a source-to-site distance of 15 km for earthquake magnitudes ranging from **M**5 to **M**9.

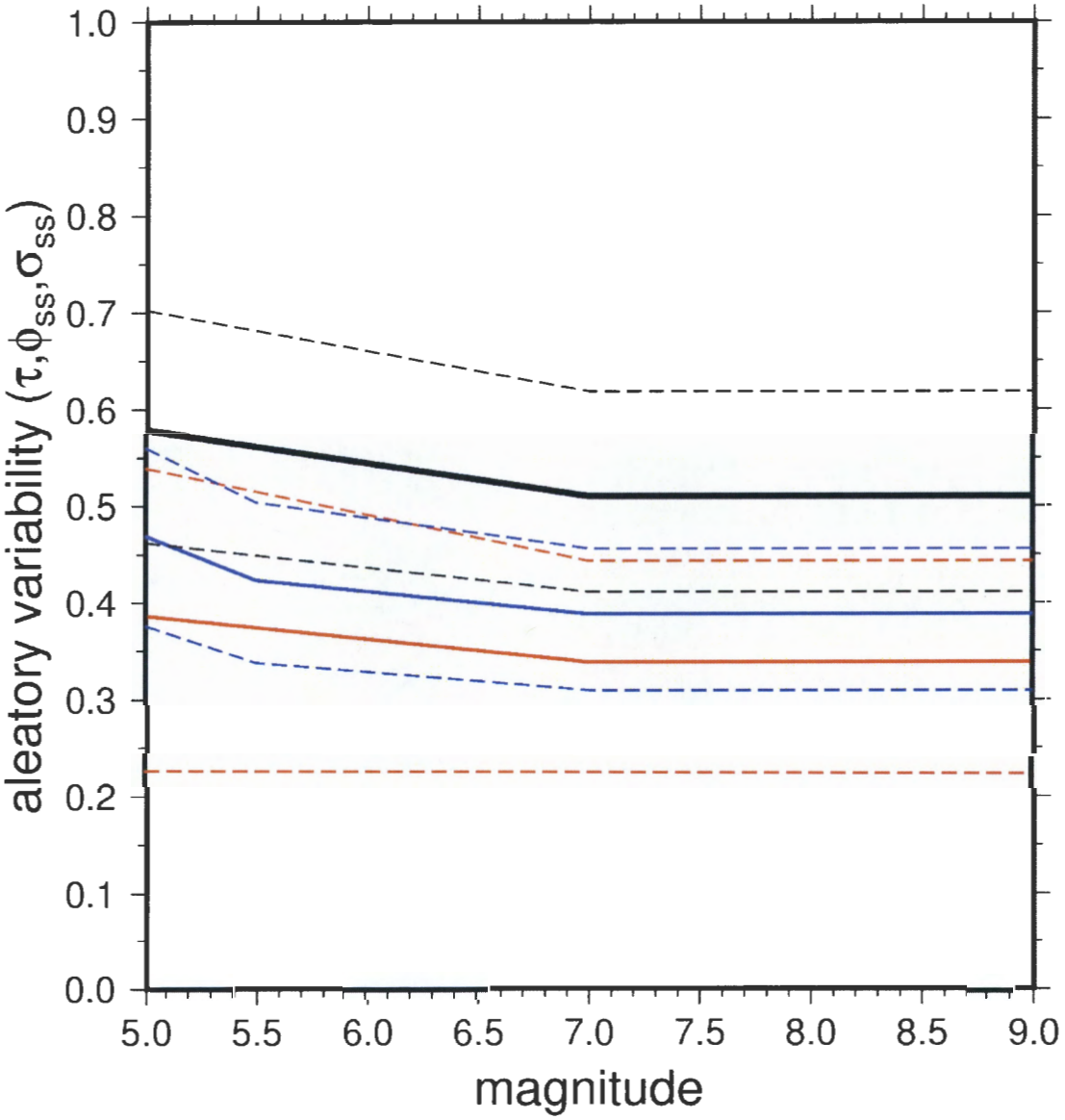

Figure 3.2-2. Low, central, and high values for the three components of aleatory variability [τ(red), φ_{SS} (blue), σ_{SS}(black)] as a function of magnitude. Solid lines represent the median variability and dashed lines represent the upper and lower bounds.

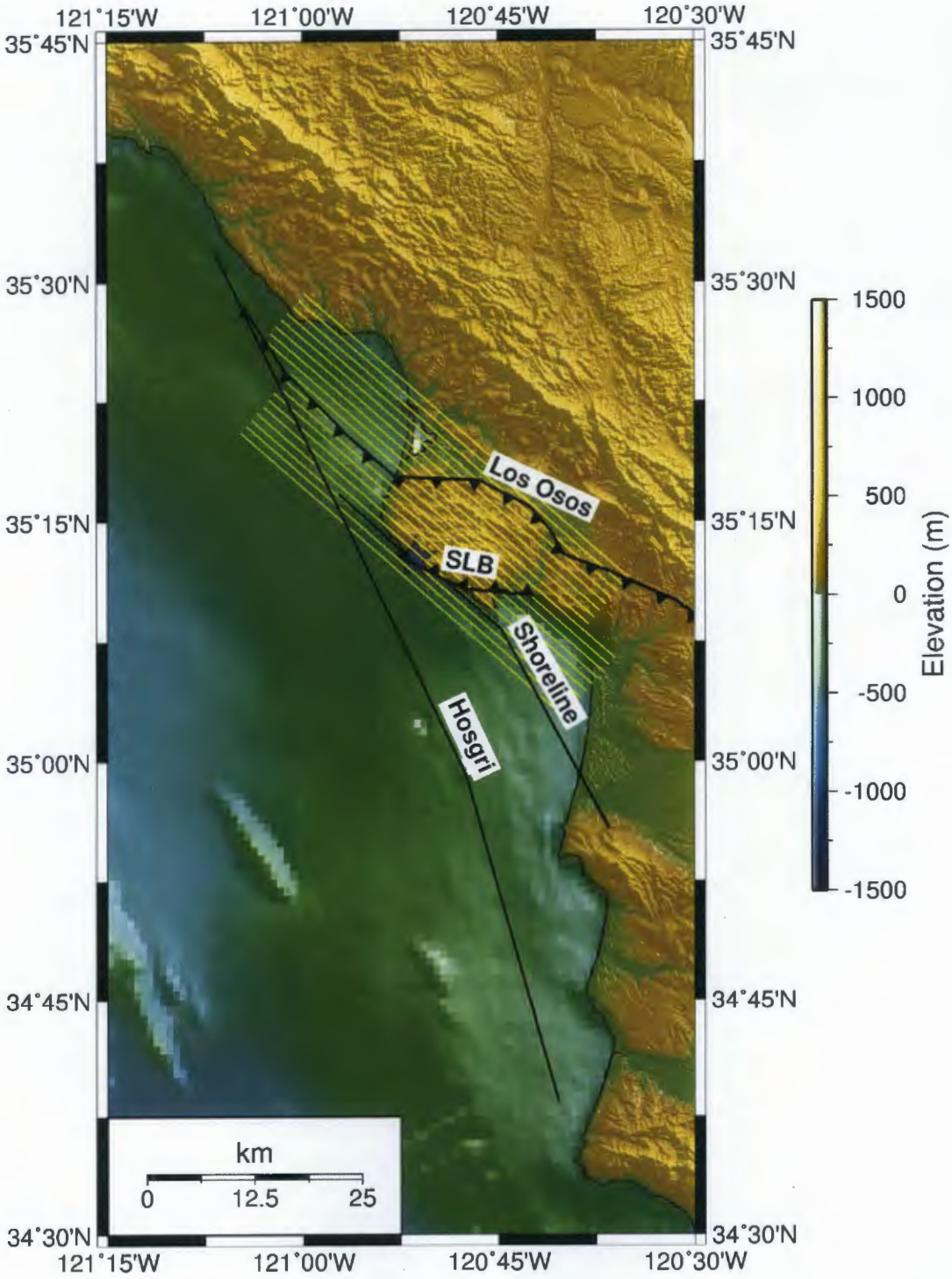

Figure 3.3-1. Four local faults (black lines) and virtual faults (yellow lines) used in the NRC staff's confirmatory analyses.

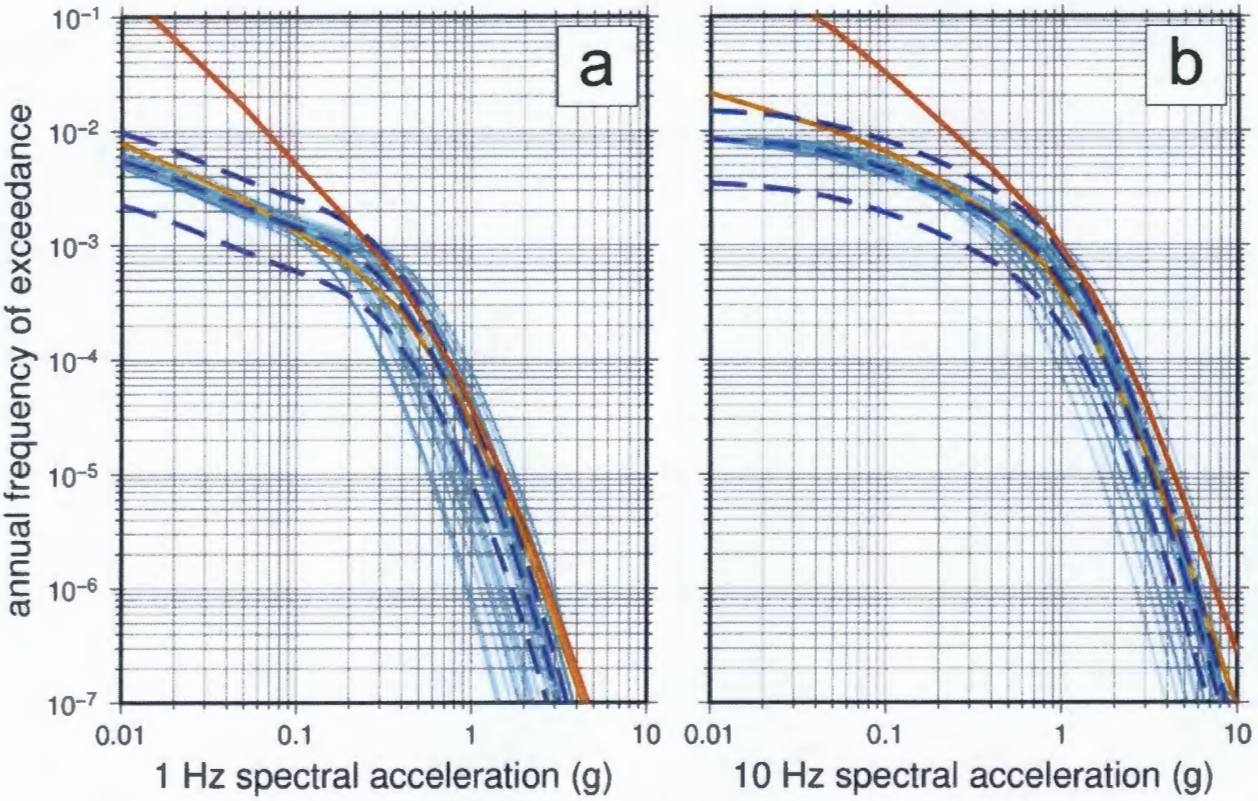

Figure 3.3-2. Results of the NRC staff's 1 Hz (a) and 10 Hz (b) confirmatory analysis for the Hosgri fault, assuming the H90 fault geometry model, a maximum magnitude of 7.4, a fault length of 107 km, a width of 12 km, an equivalent Poisson's ratio of 1.2, and fault slip rates of 0.7, 1.7, and 2.6 mm/yr. Individual analyses, assuming median slip rate, for each GMPE shown by thin light blue lines, staff mean confirmatory results for three fault slip rates shown by dashed blue lines, licensee's mean result in orange line, and the licensee's total mean result for 1 Hz (a) and 10 Hz (b) shown by the red line.

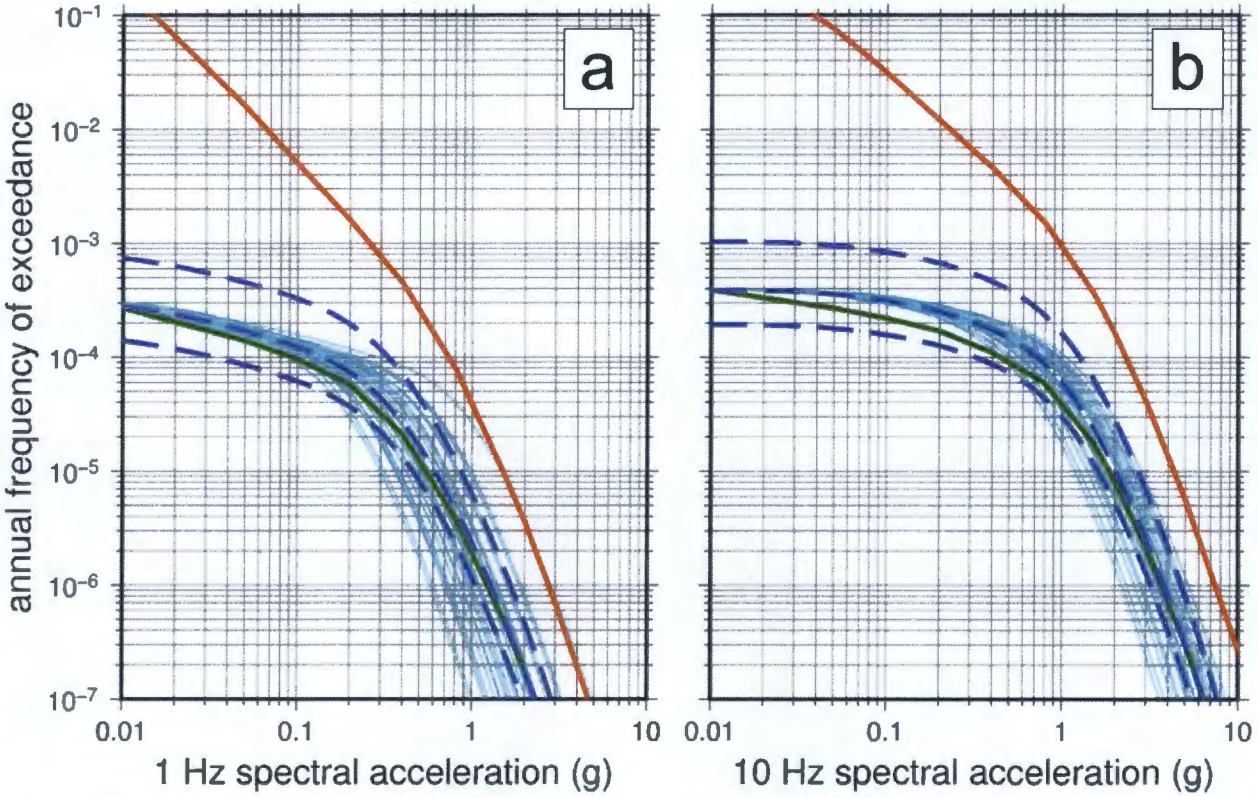

Figure 3.3-3. Results of the NRC staff's 1 Hz (a) and 10 Hz (b) confirmatory analysis for the Shoreline fault, assuming the OV-01 fault geometry model, a maximum magnitude of 6.7, a fault length of 51 km, a width of 12 km, and fault slip rates of 0.03, 0.06, and 0.16 mm/yr. Individual analyses, assuming median slip rate, for each GMPE shown by thin light blue lines, staff mean confirmatory results for three fault slip rates shown by dashed blue lines, licensee's mean result in orange line, and the licensee's total mean result for 1 Hz (a) and 10 Hz (b) shown by the red line.

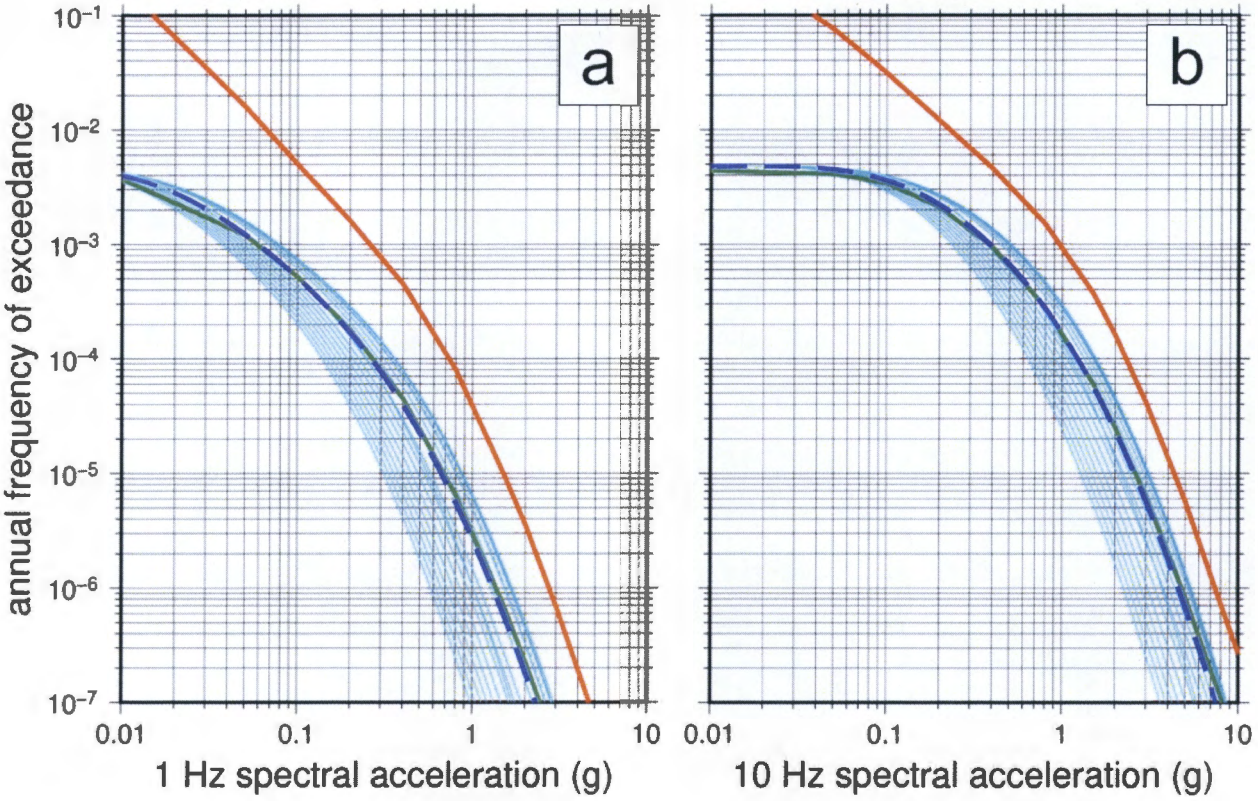

Figure 3.3-4. Results of the NRC staff's 1 Hz (a) and 10 Hz (b) confirmatory analysis for the virtual faults (yellow lines in Figure 3.3-1). Mean hazard curves for each of the virtual faults shown by thin light blue lines, overall mean result shown by dashed blue line, licensee's mean result by green line, and the licensee's total mean result for 1 Hz (a) and 10 Hz (b) shown by the red line.

Figure 3.4-1. Aerial view of the DCPP site location, basemap from Google Maps. Red squares indicate location of ESTA 27 (south of Turbine Building) and ESTA 28 (north of the Turbine Building).

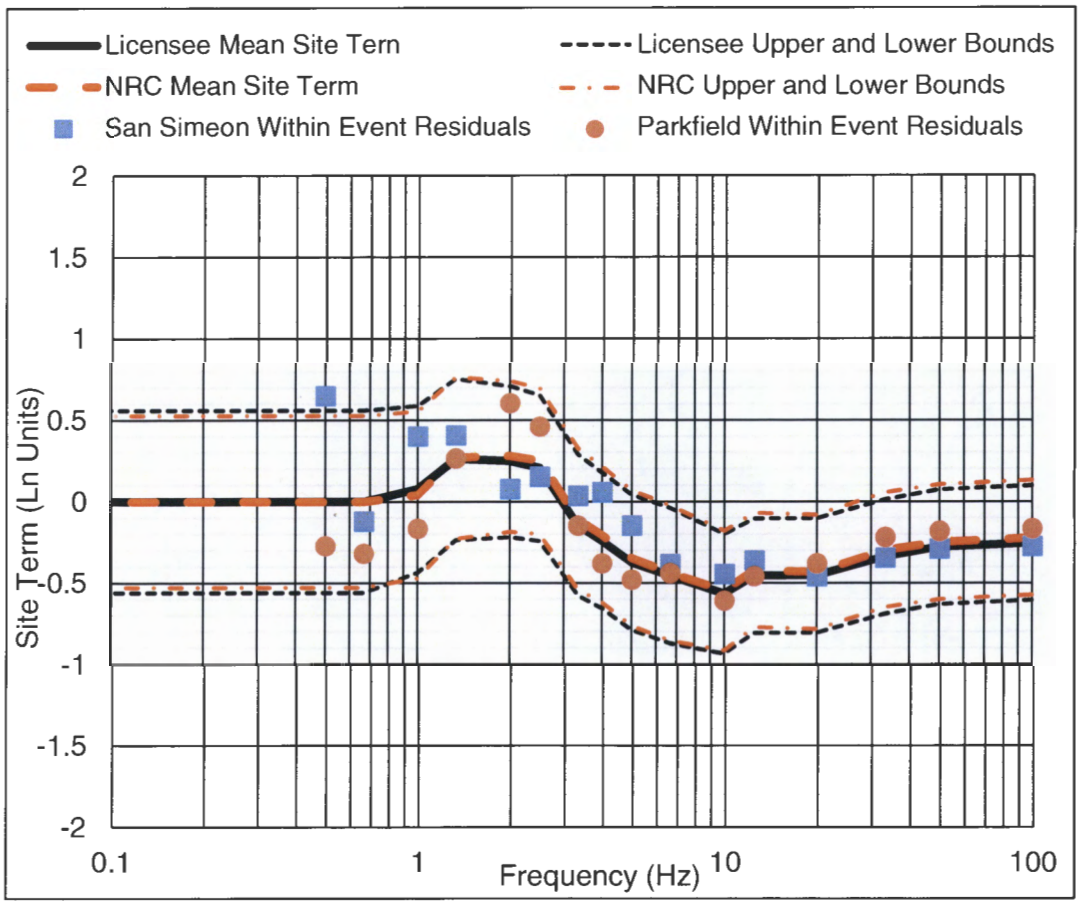

Figure 3.4-2. Empirical site term for the DCPP, showing the results of NRC staff's confirmatory analyses (red lines) and the licensee's analyses in PG&E (2015b).

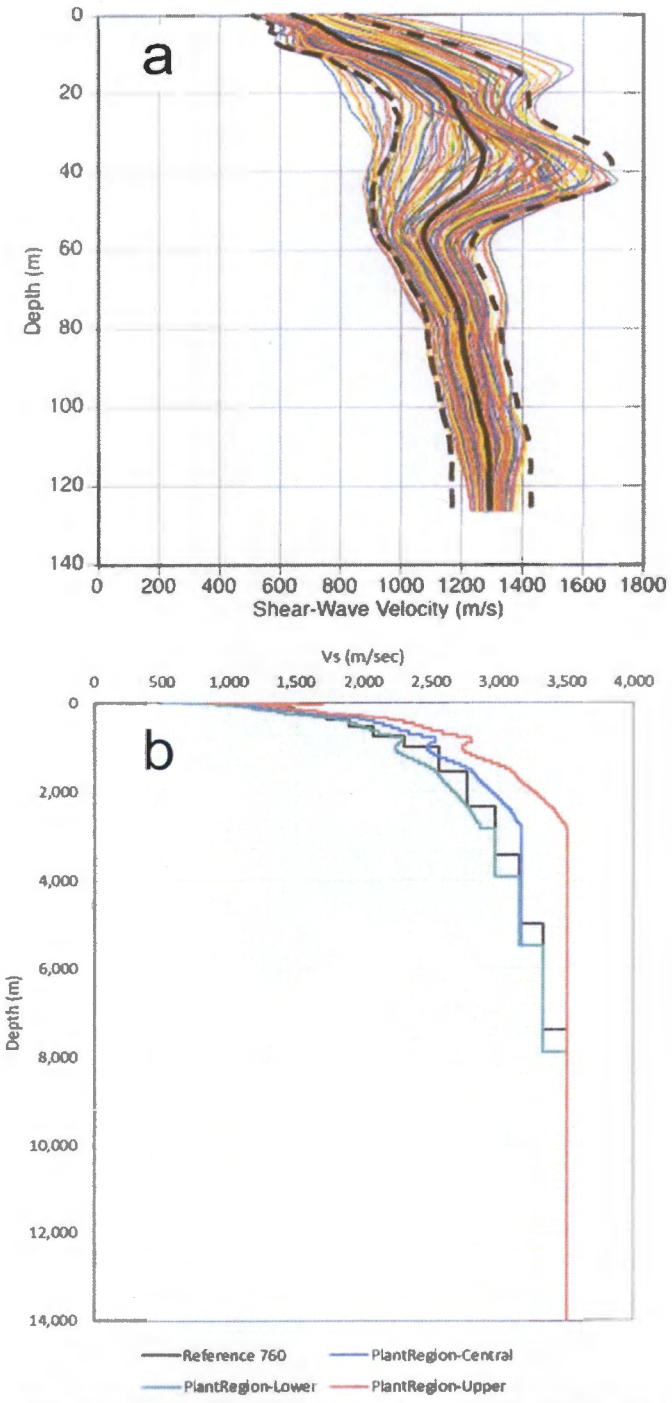

Figure 3.4-3. (a) Shear wave velocity profiles (colored lines) beneath the DCPP power block and turbine building region. Heavy black curves show the central, upper, and lower profiles. From Figure 2-2 of PG&E (2015d). (b) Comparison of the host V_S profile (labeled Reference 760) and the central, upper, and lower profiles for the target, from Figure 2.3 of PG&E (2015d).

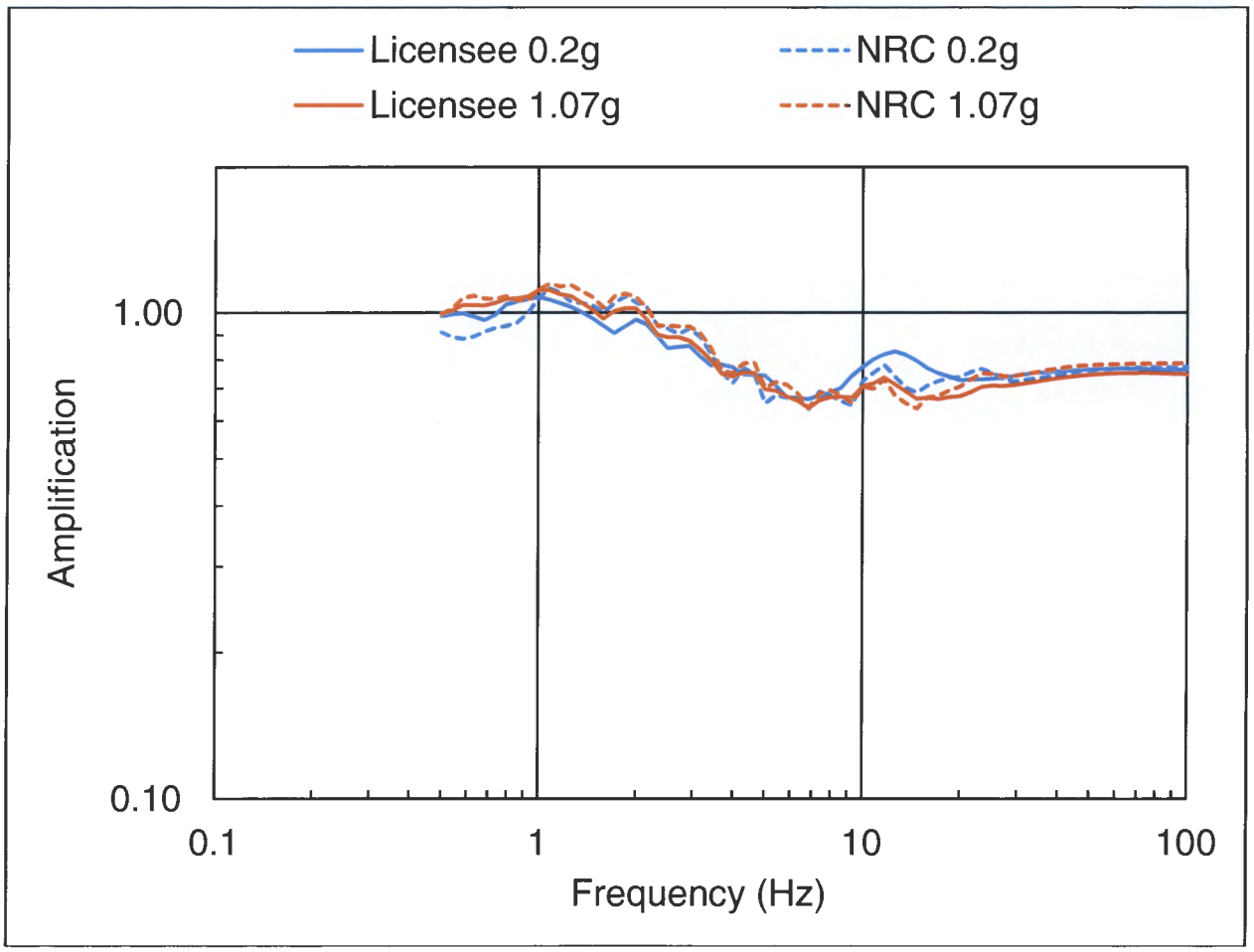

Figure 3.4-4. Comparison of analytical site terms for SWUS reference rock (760 m/s) with peak ground accelerations of 0.2g and 1.07g.

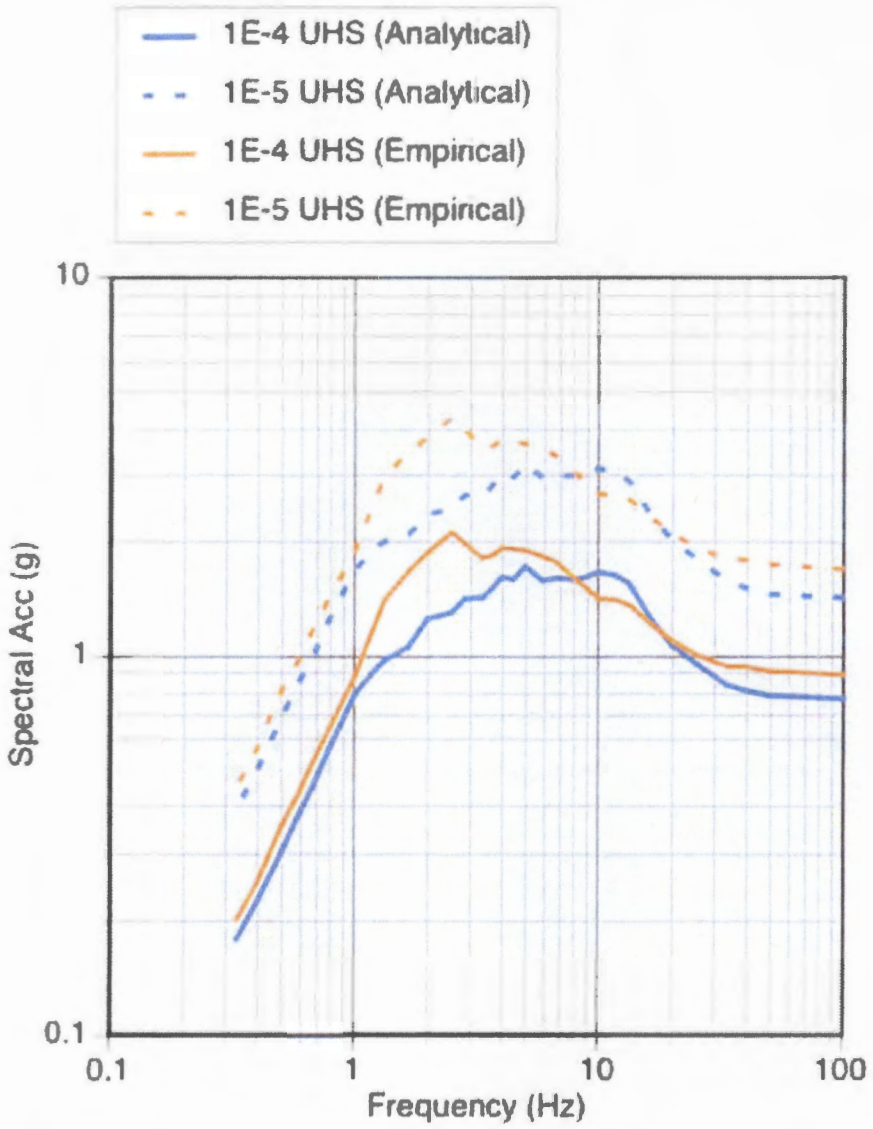

Figure 3.4-5. Licensee's sensitivity analysis of the Uniform Hazard Spectra to the site term approach, from PG&E (2015d).

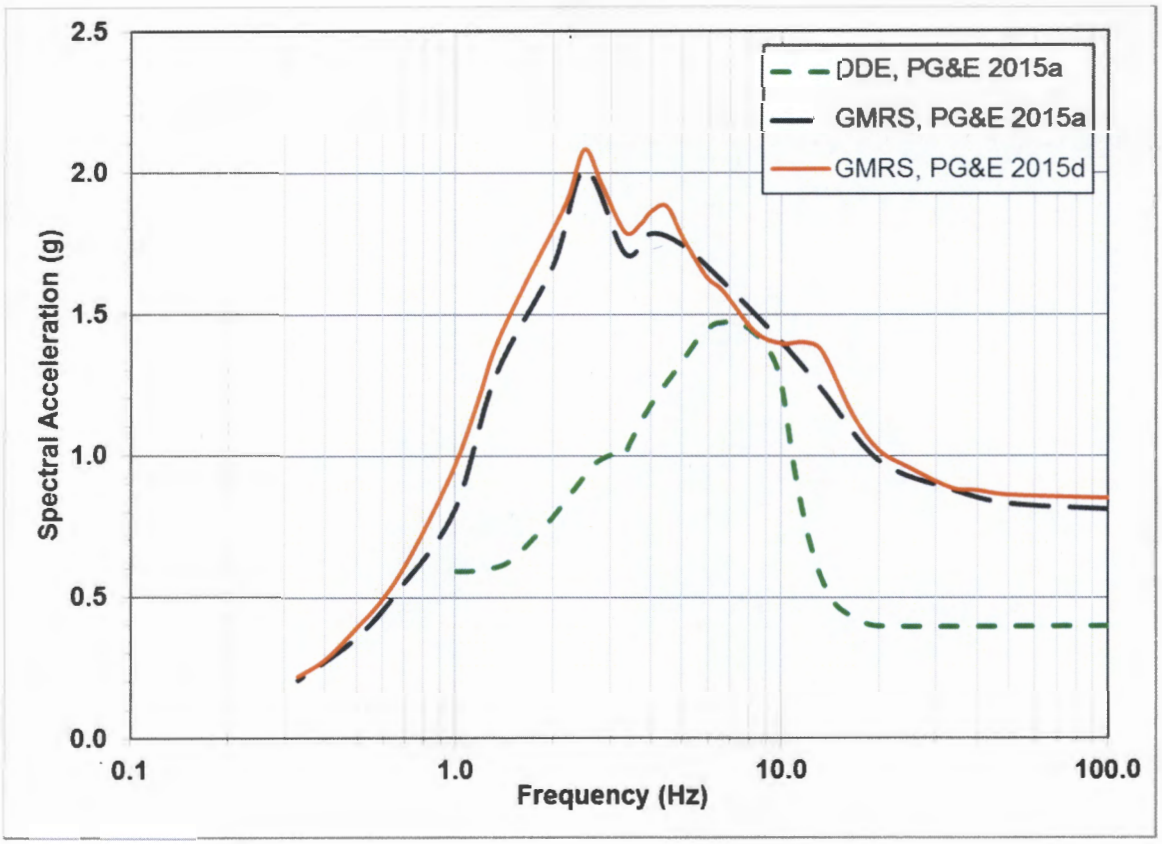

Figure 3.5-1. Initial Ground Motion Response Spectrum (GMRS; black dashed line) and Double Design Earthquake (i.e., SSE; green dashed line) from SHSR for DCPP (PG&E, 2015a). Revised GMRS (red solid line) from PG&E (2015d).

If you have any questions, please contact me at (301) 415-1617 or at Frankie.Vega@nrc.gov.

Sincerely,

/RA/

Frankie Vega, Project Manager
Hazards Management Branch
Japan Lessons-Learned Division
Office of Nuclear Reactor Regulation

Docket Nos. 50-275 and 50-323

Enclosure:
Staff Assessment of Seismic
Hazard Evaluation and Screening Report

cc w/encl: Distribution via Listserv

DISTRIBUTION:

PUBLIC
JHMB R/F
RidsNrrDorlLPL4-1 Resource
RidsNrrPMDiablo Canyon Resource
RidsNrrLASLent Resource
BSingal, NRR
FVega, NRR
BTitus, NRR
MDudek, NRO
GBowman, NRR
RidsAcrsAcnw_MailCTR Resource

ADAMS Accession No. ML16341C057 ***via email**

OFFICE	NRR/JLD/JHMB/PM	NRR/JLD/LA	NRO/DSEA/RGS/BC*	OGC	NRR/JLD/JHMB/BC(A)	NRR/JLD/JHMB/PM
NAME	FVega	SLent	MDudek	BHarris	GBowman	FVega
DATE	12/09/2016	12/08/2016	12/05/2016	12/13/2016	12/20/2016	12/21/2016

OFFICIAL RECORD COPY